A NEAR-FIELD INVESTIGATION OF TWO UNIFORMLY PERIODIC LOOP ARRAYS

By

Ersan Tezmen

United States Naval Postgraduate School

THESIS

A NEAR-FIELD INVESTIGATION OF TWO UNIFORMLY PERIODIC LOOP ARRAYS

by

Ersan Tezmen

December 1970

A Near-Field Investigation of Two Uniformly Periodic Loop Arrays

by

Ersan Tezmen
Lieutenant, Turkish Navy
B.S., Naval Postgraduate School, 1970

Submitted in partial fulfillment of the requirements for the degree of

MASTER OF SCIENCE IN ELECTRICAL ENGINEERING

from the

NAVAL POSTGRADUATE SCHOOL
December 1970

ABSTRACT

The k-β diagrams for two different uniformly periodic loop antenna arrays are determined from measured near field amplitude and phase distributions of waves traveling on the structures.

It is found that there are frequency regions where these structures function as effective radiators. The directional characteristics of the radiated fields depend upon the relative phase and amplitude distributions of the near fields.

The k-β diagrams of these periodic antennas are used to predict the behavior of their tapered broadband versions.

The results of this study demonstrate that providing appropriate conditions of phasing are met, backfire radiation can be established and, in turn, a successful broadband antenna can be designed.

TABLE OF CONTENTS

I. INTRODUCTION -- 6

A. HISTORICAL BACKGROUND -------------------------- 6

B. THE k-β DIAGRAM, ITS DETERMINATION AND APPLICATION TO PERIODIC STRUCTURES ------------16

1. Interpretations of k-β diagrams -----------16

2. Techniques for obtaining k-β diagrams -----19

a. Theoretical Determination of k-β diagrams --------------------------------19

b. Experimental Determination of k-β diagrams --------------------------------22

II. MEASUREMENT CONSIDERATIONS AND DESCRIPTION OF EXPERIMENT SET-UP ----------------------------------25

A. THE AMPLITUDE DISTRIBUTION MEASUREMENT --------25

B. THE RELATIVE PHASE MEASUREMENT ----------------27

III. EXPERIMENTAL RESULTS AND INTERPRETATION OF DATA ---34

A. TYPE A - UNIFORM ARRAY (UNREVERSED) -----------34

B. TYPE B - UNIFORM ARRAY (REVERSED) -------------47

IV. CONCLUSIONS AND RECOMMENDATIONS -------------------57

APPENDIX A: A BROADBAND PRINTED CIRCUIT BALUN ---------60

BIBLIOGRAPHY ---63

INITIAL DISTRIBUTION LIST ----------------------------65

FORM DD 1473 ---67

LIST OF ILLUSTRATIONS

Figure		
I-1	Log-periodic toothed structure (self-complementary)	7
I-2	Log-periodic dipole construction	10
I-3	Current distribution on a circular loop one wavelength in circumference	14
I-4	Dispersion diagram of free space	16
I-5	Important regions of a representative k-β diagram	17
I-6	Transmission line loaded with a periodic circuit	21
II-1	Block diagram of equipment set-up for measurement of amplitude distribution	26
II-2	Details of the near-field sampling probe	28
II-3	Block diagram of equipment set-up for measurement of relative phase distribution	30
III-1	Type A - Uniformly periodic loop antenna (unreversed)	35
III-2-8	Measured amplitude and phase distribution for Type A array	39-45
III-9	The k-β /Attenuation diagram for Type A array	46
III-10	Type B - Uniformly periodic loop antenna (reversed)	48
III-11-16	Measured amplitude and phase distribution for Type B array	50-55
III-17	The k-β /Attenuation diagram for Type B array	56
A-1	Illustration of the construction of a printed circuit balun	61

ACKNOWLEDGEMENT

The author wishes to express his appreciation to Professor R. W. Adler for the invaluable aid and counsel which he has offered during the preparation of this thesis.

I. INTRODUCTION

A. HISTORICAL BACKGROUND

In practice, there are usually space and cost limitations on antenna systems. As a result, it is often necessary to design antennas which have almost identical operational characteristics over a range of frequencies. Research to develop antennas whose performance is almost independent of frequency was carried out at the University of Illinois in the period from 1955 to 1958. Consequently, many different unconventional structures were produced. Professor V. H. Rumsey, then antenna laboratory director, noticed that the features which result in frequency dependence are the "characteristic lengths" of the structure. Antenna performance, with regard to both input impedance and ratiation pattern, is characterized by the antenna dimensions measured in wavelengths. Thus, Rumsey concluded that the structural feature required for frequency independent operation is the absence of characteristic lengths, hence the structure should be completely described by angles. He conceived of the "angle concept", which is, that a structure whose shape is defined by angles alone, with no characteristic lengths, should be a frequency independent structure.

Many different kinds of structures were tested which met this angle concept requirement. In all cases the bandwidth was limited because of truncation effects, i.e., the

currents were not negligible at the point of truncation. R. H. DuHamel, one of the workers at Illinois, realized that if the currents on the structure fall off with distance from the feed point more rapidly than usual, then they could be neglected at the point of truncation. His method for accomplishing this was to introduce discontinuities, for example, teeth in the fins of a bow-tie structure, in an attempt to increase the radiation and the decay of current. DuHamel decided that he should follow Rumsey's angle concept as far as possible during design of this particular structure. Consequently, he cut the teeth along circular arcs and let the length of the arcs be determined by an angle (see Figure I-1.).

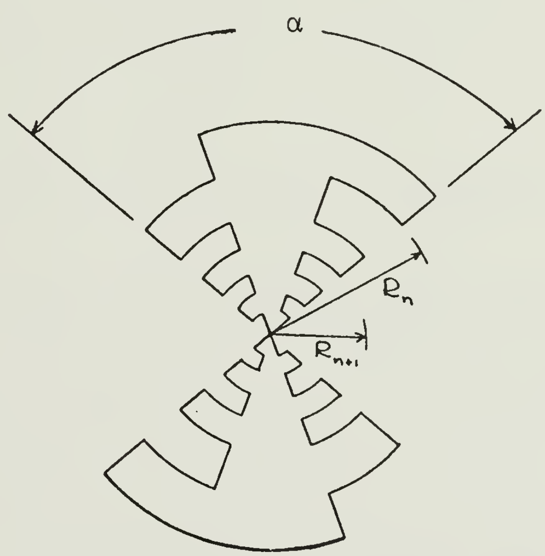

Figure I-1.

Log-periodic toothed structure (self-complementary)

This did not fix the tooth spacing, since the latter could not be specified by angles only. In trying to decide what spacing to use on the teeth, DuHamel noticed on the equi-angular spiral, which was a successful structure, along a line drawn from the center outward, the spacing from one conducter to the next were in a constant ratio. Hence he considered spacing the teeth in his structure at constant ratio.

This was accomplished by choosing the radii of the circular arcs forming the corresponding parts of the successive teeth such that they were in a constant ratio, $R_{n+1}/R_n = \tau$. He also expected that the structure would not necessarily be frequency-independent but the performance on an infinite structure would be identical at a discrete number of frequencies, which were related by the equations,

$$f_n = f_{n+1} \cdot \tau \qquad \text{or}$$

$$\log f_{n+1} = \log f_n + \log(1/\tau)$$

Inspection of this last equation shows that the performance is a periodic function of the logarithm of the frequency (i.e., the frequencies at which the performance is the same are spaced equally when plotted on a log scale). Thus, these types of structures were named "log-periodic" antennas.

Many structures of this type were built and tested. Some of them were successful and some of them were not.

Further details can be found in articles by Dyson [1] and Weeks [2].

The next major step was made by Isbell, a laboratory assistant working with DuHamel, when he invented the log-periodic dipole array. His work was motivated by the desire to develop broadband arrays of more conventional construction. Previous to Isbell's investigation, DuHamel had recognized that the sheet-metal structures could be simulated with wires or tubes. Thus Isbell decided to build and test an antenna array constructed of conventional wirelike elements with the length of the elements being determined by an angle, α, as before, and the spacings such as to give log-periodic type of behavior, (i.e., successive distances between the apex and the elements were in a constant ratio, $R_{n+1}/R_n = \tau$). At this point the big question was how to excite the elements in this array. By previous experience, Isbell, decided that in order to simulate the toothed structure, the dipoles should be connected to a parallel-wire transmission line in such a manner that the successive elements come out from the line in opposite directions. In addition, the consecutive dipoles should be connected with 180 degree phase shift to achieve a successful log-periodic structure. He accomplished this with the type of construction indicated in Figure I-2. When this 180 degree phase shift was not added, unsuccessful designs resulted. Experiments with the structure showed that in a certain range of values for τ and α, the structure was broadband with a unidirectional pattern. Isbell

also demonstrated that most of the radiation was coming from those dipole elements which were in the vicinity of a half wavelength long and that the currents and voltages at the large end of the structure were negligible within the operating band of frequencies. Finally, it was shown once again that the operating band frequencies was limited at the high end of frequencies corresponding to the size of the smallest elements and on the low end by the frequencies at which the largest element is about a half wavelength long [3].

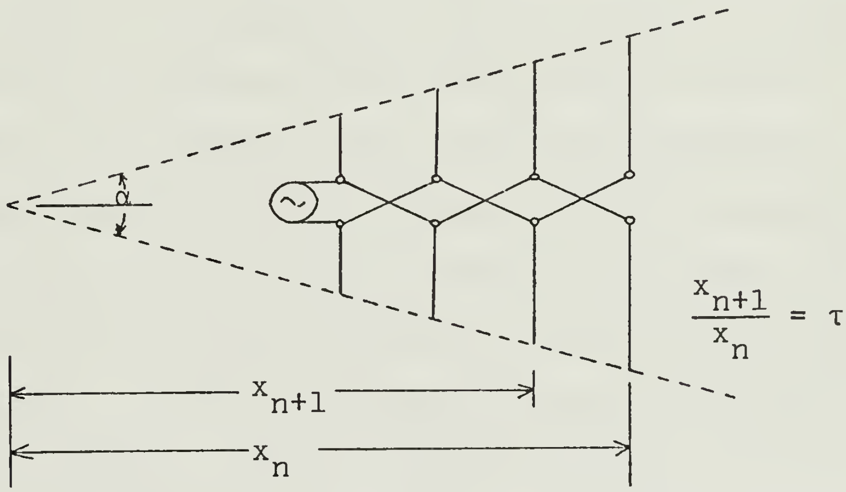

Figure I-2

Log-periodic dipole construction

A mathematical analysis of the LP dipole antenna was made by R. L. Carrel [4, 5]. He divided the problem into two parts. The unknown voltages and currents along the feeder constitute the interior part of the problem. Determining the unknown far fields of the dipole elements constituted the exterior part. Since the feeder determined the circuit properties of the antenna: impedance, voltage, and current, circuit techniques could be used in the solution of the interior problem. By making the assumption that the element currents were sinusoidal, Carrel computed the mutual impedances between the dipole elements and the self-impedance of each element. By using these impedance values as loads on a transmission line, he then found the input impedance, voltages, and currents on the loaded transmission line, together with the input currents at each antenna element. As the last part of the problem, with the specific values for the magnitude and phase of the currents in the antenna elements, the radiation pattern was calculated. All of these calculations were carried out on a digital computer, and the results compared with corresponding values from experimental models. The computer output agreed with the experimental results perfectly. As a result of his work, Carrel presented a set of design curves which allowed one to choose the dimensions of a structure in order to meet specified design objectives.

In spite of a massive research effort, it is still not known how one can assure desired performance of various

types of log-periodic antennas. Log-periodic design has largely been an art, an application of empricism based on intuition, and not really a science. Most of the papers written on the subject are experimental in nature and the theoretical development of the LP antenna design is very much in its infancy. Mittra and Jones [6] applied the same principles, as Carrel did, to various types of LP antennas. As mentioned before, this approach although quite useful for some LP antennas, does not cover all possible configurations. Another approach which views the LP device as a tapered version of a "uniform" periodic structure was first presented by Mayes, Deschamps and Patton [7]. They suggested that a knowledge of the near-field properties of the uniformly periodic structure whose geometry is the counterpart of that of the log-periodic device may lead to a better understanding of the elements which govern successful frequency independent performance.

If β is the phase constant of a wave traveling along the structure and k $=2\pi/\lambda$ is the free space wave number, the line of demarcation between slow and fast waves is defined as $\beta = k$; the wave being slow for $\beta > k$, fast for $\beta < k$. Backfire radiation (radiation directed toward the point of excitation) was believed to be the result of a space wave traveling along the structure in the direction opposite to the phase progression of currents in the feed line. It was further considered that the backward-traveling wave was due to the existence of backward space harmonics in the

spectrum of the periodic structure. The periodic structure should produce only waves which are quite slow at the frequencies where radiation is not intended. At frequencies where radiation is desired, one or more of the space-harmonic waves should be fast. Thus, for the tapered LP structure, a feeder wave progresses toward the active (radiating) region under slow wave conditions. According to this theory, the dominant space harmonic in the active region is one which propagates in the backward direction.

The near-field characteristic of fundamental interest, therefore, is the relative phase velocity or, the k-β relationship. With the uniformly period structure, the k-β relation is observed as a function of frequency. Extensive use has been made of k-β (Brillouin) diagrams by many investigators. Mittra and Jones [8] calculated the k-β diagrams for unreversed and reversed uniform dipole arrays where only a single mutual admittance term between the antenna elements was retained (mutual admittance between widely separated elements can be neglected). In the unreversed case the k-β diagram began with a slow-wave region and shifted into a fast-wave region (which is radiation region) near the resonance point of the dipoles. This structure was tapered, showed large truncation effects and considerable frequency dependence. The reversed dipole array, which is the untapered counterpart of the well-known log-periodic dipole array, had a k-β diagram that was essentially the same. The only difference was, the attenuation was considerably larger than in the previous case. The

tapered form of this structure was a successful broadband antenna. At the conclusion of this work, they emphasized that to get a well-behaved log-periodic antenna, one had to start with its successful untapered counterpart, this not being a sufficient but a necessary condition.

In September of 1967, James E. Lindsay, Jr. [9] discussed the possibility of the application of loop elements of one wavelength circumference in a Yagi-Uda array where there is a 1.8 db gain advantage over a conventional dipole yagi of equivalent length. For a loop of approximately one wavelength in circumference, the current distribution is shown in Figure I-3, and it has lossy transmission line characteristics. This is easily visualized by considering

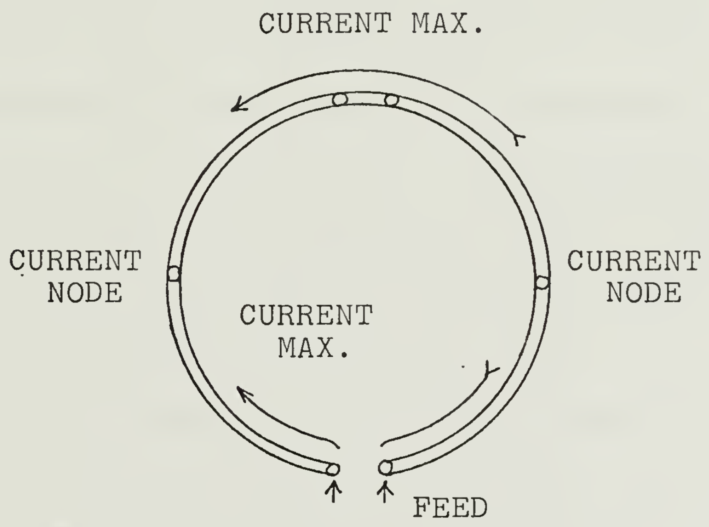

Figure I-3.

Current distribution on a circular loop one-wavelength in circumference.

the loop to be a deformed, shorted one-half wavelength

parallel-wire lossy transmission line bent into a circle. The loop will have a far field radiation pattern which is maximum broadside to the plane of the loop (i.e., along the axis of the loop). The polarization will be linear and parallel to an imaginary line connecting the two current nodes. The directivity of a one-wavelength loop is approximately 1.8 dB above a one-half wavelength dipole. As mentioned before, this differential of 1.8 dB also appears when a parasitic array of loops is compared to a Yagi-Uda array. A log-periodic antenna has been designed by the Taco Co., using conventional log-periodic dipole theory and replacing half wavelength dipoles with full wavelength loops. A log-periodic dipole array also was made for comparison purposes. The results were quite encouraging with higher gain and better radiation pattern characteristics than those from conventional log-periodic dipole arrays. In addition, it had broadband impedance characteristics. No attempt was made to analyze this log-periodic loop array and the operating bandwidth chosen was quite small, approximately 50 percent.

The development of the log-periodic concept has been traced and the importance of uniformly periodic arrays as counterparts of log-periodic arrays was pointed out. But it is obvious that there is an infinite variety of log-periodic structures. The obvious advantages of log-periodic loop arrays as mentioned in the last part of this section, encouraged this investigation.

B. THE k-β DIAGRAM, ITS DETERMINATION AND APPLICATION TO PERIODIC STRUCTURES

1. Interpretation of k-β Diagrams

The purpose of this thesis is to study uniformly periodic loop array antennas and from this to get some knowledge about their logarithmically periodic derivations. It is largely an experimental effort. The k-β diagram which was obtained experimentally is used as a main analytic tool to accomplish this goal.

As mentioned before, the k-β diagram is obtained by plotting the free-space phase constant, k, versus the structure phase constant, β, (or kd versus βd, where d is the spacing between the antenna elements). For free-space propagation, $k = \beta$, the diagram has the form of Figure I-4.

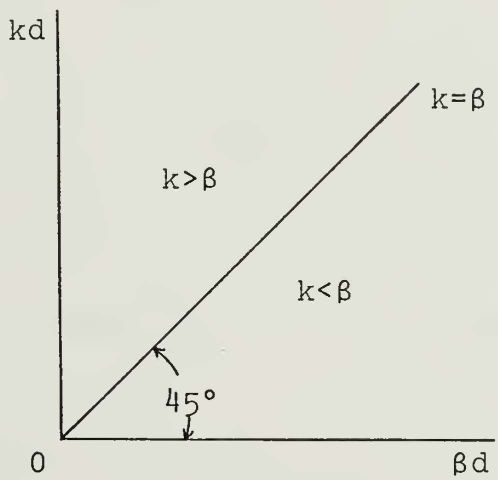

Figure I-4.

Dispersion diagram of free space.

The k-β diagram for a periodic structure can be separated into three frequency regions. This is illustrated by an example in Figure I-5.

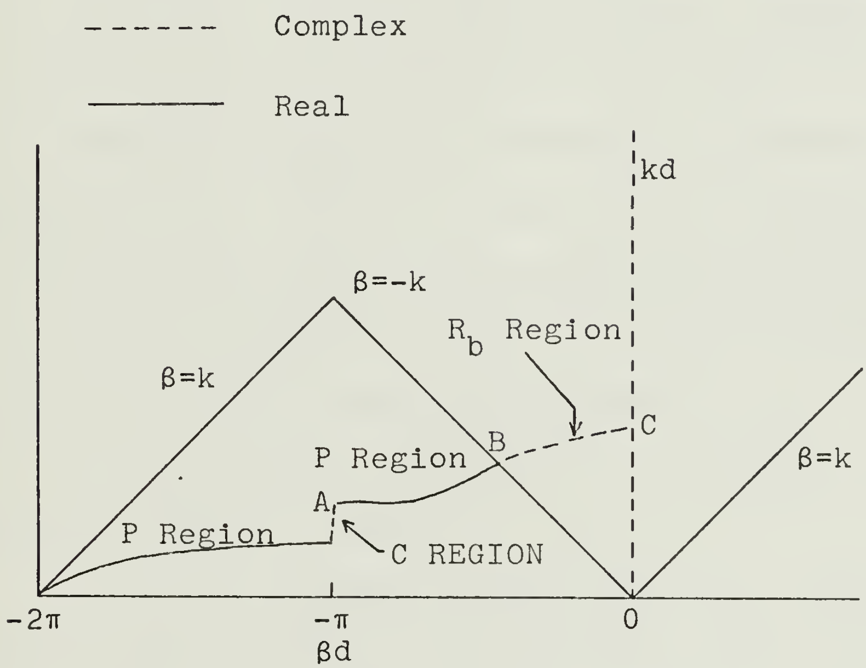

Figure I-5.

Important regions of a representative k-β diagram.

P (Propagation) region: The phase constant β in this region is real. That is, the wave on the structure suffers from little or no attenuation for this band of frequencies. This region corresponds to the excitation or transmission line region in log-periodic arrays.

C (Complex or Imaginary) region: The phase constant is complex and occurs at $\beta d = -\pi$. This creates a

stopband where the attenuation is high but coupling to space is poor.

R (Radiation) region: The phase constant is once again complex but this time it occurs well away from $\beta d = -\pi$. Here, the array is a very efficient radiator. The R region can also be divided into two regions, R_b and R_f. Region R_b denotes radiation in the backward direction; i.e., radiation toward the feed-point. R_f denotes forward radiation; i.e., radiation away from the feed-point. All of the successful log-periodic antennas have an R_b region. To date there have not been any successful log-periodic antennas built which have an R_f region.

The angle of radiation for a periodic structure is given by $\cos\theta = \beta d/kd$.

If the radiation occurs when $\beta = k$, the angle θ then is zero and this is an R_f region. But if the radiation occurs near the line $\beta = -k$, the angle θ is π and this is an R_b region, and is indicative of a potential broadband antenna if appropriately tapered.

To sum up, starting from small values of k, the untapered antenna must have a continuous P region then move into an R_b region. If the coupling to space for the wave in R_b region is very effective, the k-β properties of the structure beyond the R_b region are of no interest. However, if the P region is interrupted by a C or R_f region, ahead of the R_b region, the tapered configuration will be a potentially unsuccessful broadband antenna.

A properly designed log-periodic structure acts as a continuous impedance transformer and converts the energy from the source into radiative power. On the other hand, structures with P-R_f or P-C regions create large standing waves because of reflections into the source. Therefore structures with P-R_f and P-C characteristics are usually unsuitable as broadband log-periodic antennas. Hence, the antenna in Figure I-5 would be a poor broadband structure.

2. Techniques for Obtaining k-β Diagrams

The k-β diagram for a periodic structure is obtained either theoretically or experimentally. Both these procedures have some advantages and disadvantages. In this investigation, an experimental approach was taken.

a. Theoretical Determination of k-β Diagrams

A complete treatment of this subject is beyond the scope of this thesis, however, a brief discussion of the technique follows. The starting point for calculation of the k-β diagram is to formulate the characteristic equation for β. In general, this equation has the form,

$$F(\beta) = 0$$

where F(β) is a transcendental function of β, of the geometrical parameters of the structure and of k. Solutions of this equation are plotted as a function of k, establishing the k-β diagram.

By assuming the structure as a transmission line loaded periodically with a network and knowing its

admittance matrix [$\bar{Y}$], one can write the node equation, for example for node 1.

$$0 = \text{---} + y_{13} V_{-2} + (y_{12} + \dot{J} \text{ Cosec } kd) V_{-1}$$

$$+ (-2\dot{J} \text{ Cot } kd + y_{11}) V_o + (y_{12} + \dot{J} \text{ Cosec } kd) V_1$$

$$+ y_{13} V_2 + \text{------} \qquad \text{(I-1)}$$

Where V_m's are the node voltages and y_{in} is the mutual impedance of the loading network for node 1. It is obvious that the entire structure is periodic and has a period d. From the periodic nature of the structure it can be written that,

$$\text{if } \frac{V_1}{V_o} = e^{-\dot{J}\beta' d}$$

$$\text{where } \beta' = \beta + \dot{J}a,$$

$$\text{then } \frac{V_p}{V_q} = e^{-\dot{J}(p-q)\beta' d} \qquad \text{(I-2)}$$

where p and q are arbitrary. Substituting the above equation into Equation (I-1) and after some simplification,

$$0 = (-2j\text{Cot } kd + y_{11}) + 2(y_{12} + \dot{J}\text{Cosec } kd) \text{ Cos}\beta' d$$
$$+ 2y_{13} \text{ Cos } 2\beta' d + \text{----} \qquad \text{(I-3)}$$

or

$$\text{Cos}\beta' d = \text{Cos } kd + \frac{\dot{J}Y_{eq}}{2} \text{ Sin } kd \qquad \text{(I-4)}$$

where

$$y_{eg} = \frac{1}{Z_{11} + 2Z_{12} \text{ Cos}\beta' d + 2Z_{13} \text{ Cos } 2\beta' d + \text{------}}$$

Equation (I-4) is the characteristic equation for the configuration shown in Figure I-6. This equation was independently derived by various persons [8, 10], and can be simplified by disregarding higher order mutual impedance terms. Actually, even the calculations of each mutual impedance term are quite extensive. Therefore, arithmetic solution of the characteristic equation is handled on a computer but is still a very complex and time consuming operation. On the other hand, once the computer program is developed, it is very easy to examine different configurations of the structure, just by changing the input parameters, d and k. The equation (I-4) is directly

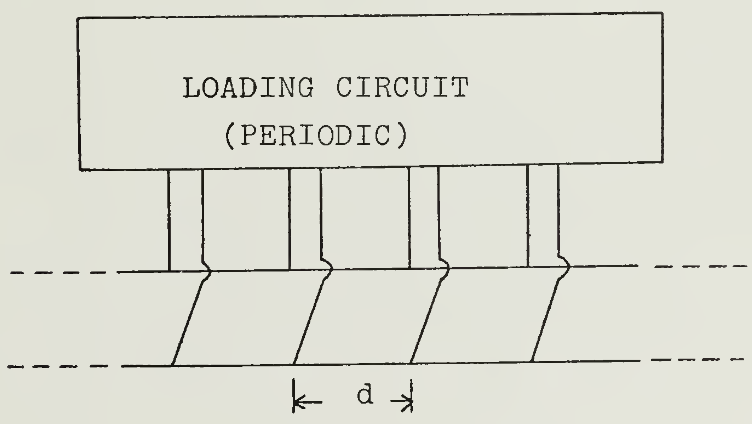

Figure I-6.

Transmission line loaded with a periodic circuit.

applicable to different arrays, such as the monopole and dipole arrays [8].

Several values of β may exist for a given value of k. Some of them can be real and others complex. It is very difficult to tell what the relative amplitudes of the various solutions will be for a given source excitation without solving the excitation problem, which is in itself difficult. Arbitrarily choosing one of the solutions may be disastrous, because another one not considered may be effective in the neighborhood of resonance, which can interfere with the accepted mode. This has been observed by Mayes and Ingerson [11]. Even if it is known that both modes are comparable in some frequency region in the uniformly periodic case, this does not mean that something definite can be said about the relative importance of the neglected modes as compared to an accepted mode in the log-periodic case. No satisfactory formulation has been developed at this time for answering these questions.

Any theoretical calculations which are performed, must be verified by experimental results. In view of these considerations, an experimental k-β investigation was undertaken.

b. Experimental Determination of k-β Diagrams

It is possible to avoid some of the difficulties and ambiguities which arise during a theoretical determination of k-β diagrams, by using an experimental technique. This method is relatively easy and gives

results which are a clear and absolute indication of characteristics of a periodic structure.

The experimental determination of k-β diagrams for a periodic array is accomplished by making near field measurements of a structure. Since the near field value is directly proportional to current on the conducting elements, one determines relative current phase and amplitude distributions.

At frequencies below which the loops are near the one wavelength resonance, the wave on the periodic structure travels with little or no attenuation. At this frequency band, the structure functions simply as a transmission line, and the propagation constant β can be determined by measuring the effective wavelength. This is accomplished by terminating the end of the structure in an open circuit, and measuring and plotting the resultant standing wave amplitude. As the frequency of the feeder wave is increased to where the loops approach wavelength resonance, the structure no longer behaves as a loaded transmission line. Here there is attenuation as the feeder wave travels along the structure away from the point of excitation. Therefore, the magnitude of the reflected wave is very small and not large enough to create a high standing wave. Consequently, the propagation constant β can no longer be determined by an observation of the standing wave pattern. Actually, the incident wave is a traveling wave, with a resultant progression of phase with distance.

To obtain the propagation constant, the difference in phase, ϕ, at two positions one period apart is divided by spacing, d. In otherwords, the slope of relative phase curve is the propagation constant β.

II. MEASUREMENT CONSIDERATIONS AND DESCRIPTION OF EXPERIMENT SET-UP

The purpose of making near-field measurements is to determine the propagation constant β of the wave on the periodic structure. Measurements were made over a 2.5 to 1 band in order to investigate the behavior of the uniformly periodic array over a wide frequency range.

The near field measurements consisted of measuring the relative amplitude and relative phase of the current flowing along the periodic structure. The methods and corresponding set-ups for making these two measurements are discussed separately below.

A. THE AMPLITUDE DISTRIBUTION MEASUREMENT

The amplitude measurement set-up, shown in Figure II-1, is a relatively simple one. More sophisticated configurations could be arranged, such as using a probe driving mechanism to get continuous sampling values.

A step-by-step explanation of the procedure used for making the near field amplitude measurements follows: Refer to Figure II-1.

1. The structure under test is fed by the signal generator through a balun (the characteristics and design procedure of this particular balun are discussed briefly in Appendix A). If the output level of signal generator is not sufficient, a power oscillator can be used.

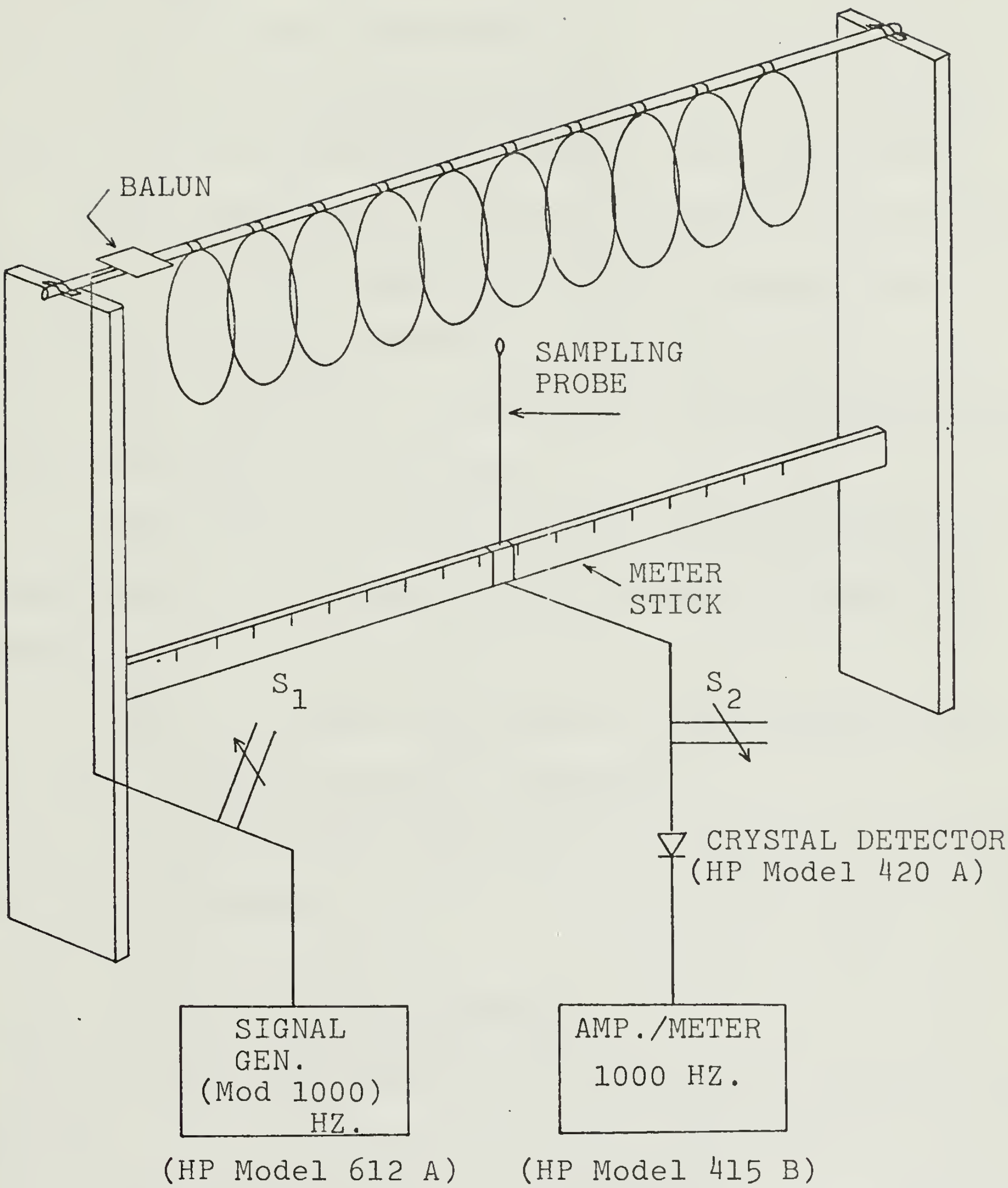

Figure II-1.

Block diagram of equipment set-up for measurement of amplitude distribution.

2. The sampling probe is positioned at the first loop. (Refer to Figure II-2, for the location of the probe with respect to the loop of the array.)

3. The output from the sampling probe is connected through a crystal detector to the 1000 cycle amplifier/ meter, being careful not to over or underdrive the crystal beyond its square-law region, otherwise, the amplitude data will not be the true value of the near field.

4. The double-stub tuners S_1 and S_2 are adjusted for maximum indication on the meter.

5. The amplitude indications for sampling increments of approximately one quarter of the structure period are recorded.

6. Data is plotted to produce a curve showing amplitude versus distance along the structure.

7. The above steps are repeated for each desired frequency of measurement.

B. THE RELATIVE PHASE MEASUREMENT

These phase measurements are based on the concept of comparison. That is, the value of the phase angle of the wave at a particular point on the structure is meaningful only if it is compared to some other point on the structure. The technique which is used, is to combine two signals of the same frequency, one of which is the sampled from the structure and the other is a phase reference signal. The relative phase of the sampled signal is determined by comparison with that of the reference. A slotted line whose

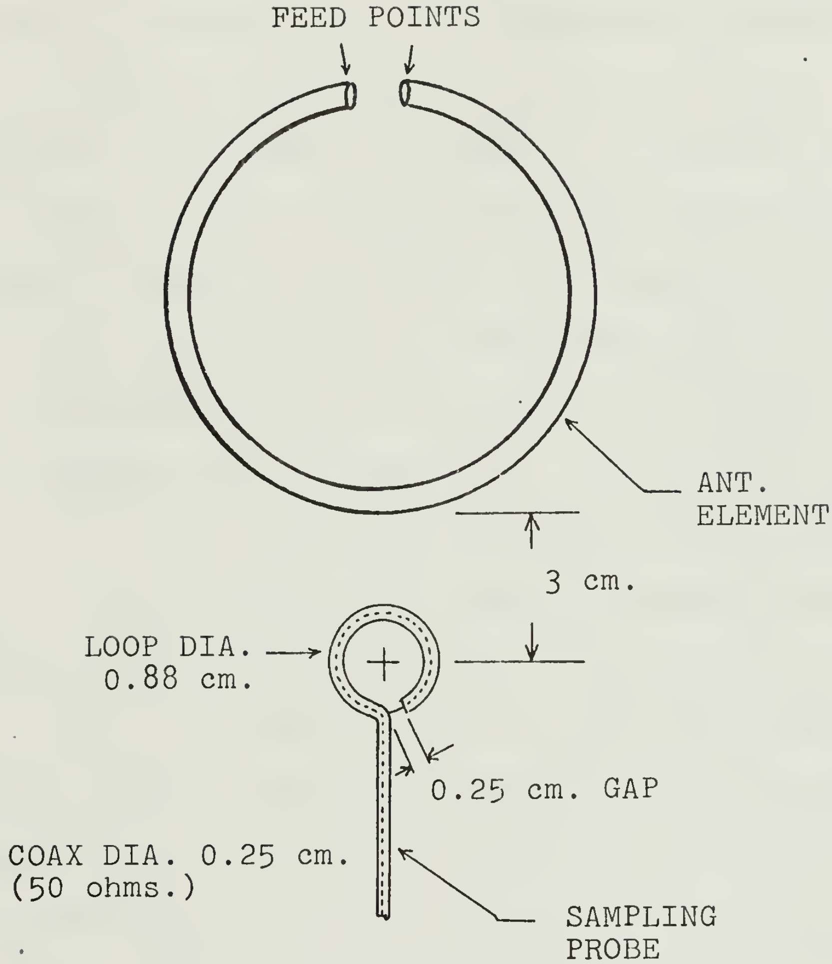

Figure II-2.

Details of the near-field sampling probe.

end is terminated in a 50 ohm matched load is used as a source of variable phase. The relative phase measurement set-up shown in Figure II-3. The reference and the test signal are applied to a T-connection, which acts as a power combiner, the output of which is the phasor sum of the two signals. This output will depend upon the relative magnitude and phase of these two signals. For a minimum, the two signals should be 180 degrees out of phase. If one is detecting minimum points, it is desirable to have the signals equal in magnitude. This is the ideal condition for minima detection but difficult to obtain in practice. As a rule of thumb, the two signals should not differ by more than about 6 db for a distinct minima detection. When the signals differ by much more than this, the minima becomes broad and difficult to locate precisely. The output of the combiner is then fed into a mixer and the resultant signals pass onto a meter for minima detection. Hence, starting from the first loop, for each increment of the sampling probe along the array, the reference probe in the slotted line should be moved by some corresponding increment to achieve the 180 degree phase difference at the T-connection inputs. The amount of shift of the minimum from that of the preceding reading represents the change in phase of the wave over the incremental movement of the sampling probe. The minimum may shift either toward (leading phase) or away from (lagging phase) the feed end of the slotted line. Sampling increments of 1.5 cm

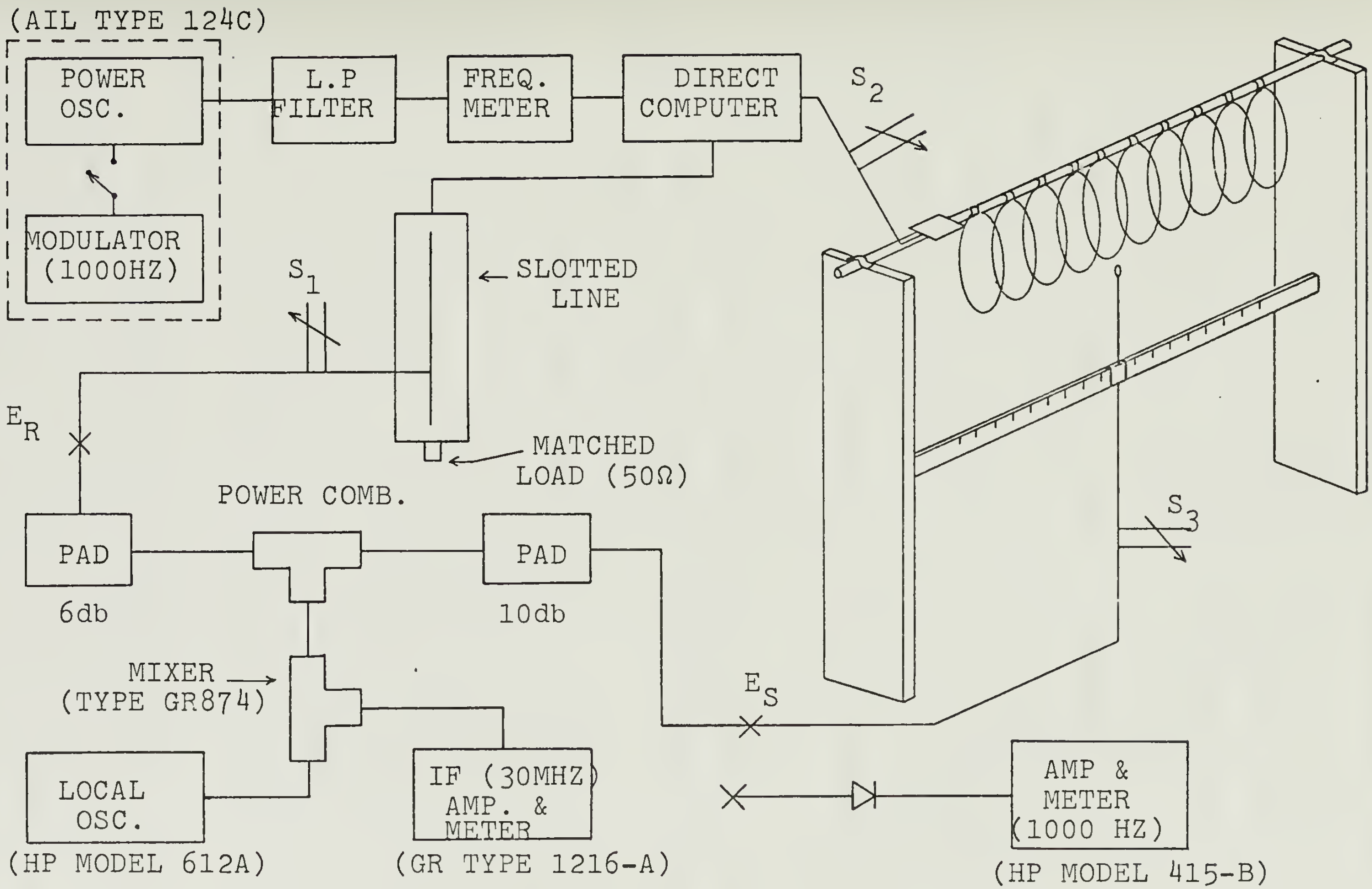

Figure II-3.

Block diagram of equipment set-up for measurement of relative phase distribution.

were adequate to make a relative phase curve for the frequency range of interest.

The amplitude distribution measurements should precede measurements of phase. In so doing, the frequencies where a sufficient standing wave pattern exists are discovered. At these frequencies, the guide wavelength can be obtained directly from the amplitude plot, otherwise, a successful determination of phase is almost impossible.

The phase need not be measured beyond the distance where the amplitude of the near field is attenuated by about 10 db. However, it is advisable to make measurements over six or seven cells even though the attenuation rate is high.

The following is a step-by-step outline of the procedure used for making the near field relative phase measurements. Refer to Figure II-3.

1. The reference signal E_R is connected from the slotted line to the metering circuit through the detector. 1000 HZ modulation is applied to the power oscillator by tuning the slotted line and adjusting S_1 (double-stub tuner), noting the signal level. E_R is reconnected to the pad and the power combiner (T-connection). A 6 db pad is used for isolation.

2. The sampling probe is positioned at the first loop with modulation still applied to the power oscillator. The sampling signal E_S is connected to the metering circuit and by adjusting S_2 and S_3, the signal level is made approximately equal to E_R. E_S is then reconnected to the pad and

power combiner. The pad provides 10 db attenuation for isolation.

3. Modulation is now removed from the power oscillator.

4. The local oscillator is tuned for the proper IF signal output from the mixer (30 MHZ above or below the RF signal frequency).

5. The slotted line probe is moved to obtain a minimum indication of the IF amplifier/meter, that is, E_S and E_R are 180 degrees out of phase. The maximum instead of minimum may also be chosen, which gives a similar result. In that case, the two signals are in phase. The corresponding location of this minimum on the slotted line is the reference point for further measurements.

6. The sampling probe is then moved to the next sampling position and the corresponding minimum is located on the slotted line. The amount of shift in the position of minimum from that of the preceding value represents the change in phase of the wave over the incremental movement of the sampling probe.

7. By repeating (6) for each increment of measurement, data is obtained for plotting a curve showing relative phase versus distance along the structure.

8. The above is repeated for each desired frequency of measurement.

At this point, it is worthwhile to note some details regarding the probe used for sampling the near field.

Referring to previous investigations [12] about near field measurements, a current-type sampling probe was chosen. The probe configuration is shown in Figure II-2.

It is essentially a circular loop enclosed by an electrostatic shield and oriented so that it is coupled primarily to the magnetic field of the antenna array, and is polarized parallel to the antenna elements. The probe is small enough to ensure the field is not seriously disturbed, but on the other hand, it is large enough to create sufficient current to produce an indication on the detection equipment. Further, it was found that when the probe was placed very close to the structure, superfluous nulls were observed in the standing wave pattern due to fields around the individual loops. A satisfactory location for the probe was found to be approximately 3 cm away from the array.

III. EXPERIMENTAL RESULTS AND INTEPRETATION OF DATA

In this section of the thesis, results of the measurements on two different uniformly periodic loop structures are presented and discussed. The only difference between these two antennas is the manner in which they are fed. The antenna elements in Type A are simply fed in shunt from a double-wire transmission line, hence, the structure incorporates no mechanism for phasing other than that which the loops themselves provide through loading of the feed line. On the other hand, for Type B, the loops are placed along an alternately transposed double-wire feed line. This method provides a 180 degree phase shift between loops.

Each antenna with its corresponding data is discussed below.

A. TYPE A - UNIFORM ARRAY (UNREVERSED)

This uniformly periodic structure consists of an array of ten identical loops, equally spaced at 6.5 cm. along a two-wire transmission line whose conductors are 2.5 cm. apart. The circumference of each loop was chosen to be equal to approximately one wavelength at a midfrequency of 800 MHZ (37.5 cm). The structure is illustrated in Figure III-1.

Figures III-2 through 8 contain the recorded amplitude and phase data for this type antenna. The k-β and

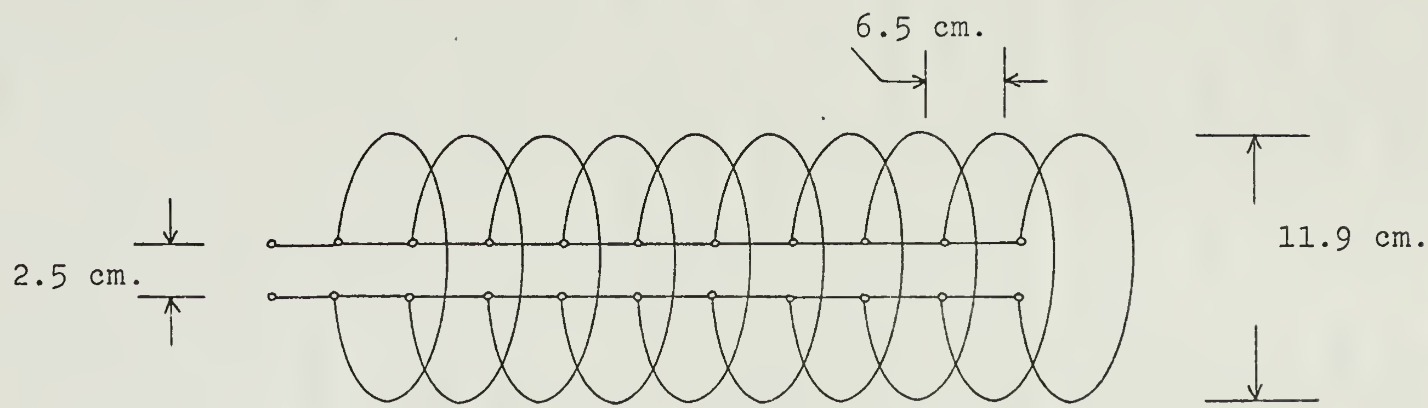

Figure III-1.

TYPE A. Uniformly periodic loop antenna (unreversed).

attenuation curves of Figure III-9, which summarize the data are derived from the amplitude and phase curves.

The points appearing on the amplitude and phase curves represents the points along the structure at which the measurements were made. The relative magnitude of near-field current in db is shown along the right ordinate and the relative magnitude of the phase in degrees along the left ordinate. The loop locations are along the abscissa, with the first loop at the extreme left. The data shown are generally those which correspond to the more significant points on the k-β curve. Each diagram represents a different frequency of operation.

Since this structure is the first on which the measured results are presented, in the discussions of the Type B structure which follow, only the data which differ significantly from those for the Type A structure, are elaborated upon.

Beginning with the amplitude plot at 500 MHZ shown in Figure III-2, it is seen that the amplitude distribution of current along the structure is of the form of a uniform standing wave. No attenuation is associated with the wave supported on the structure. The propagation constant can be determined by finding the spacing between the adjacent nulls of the standing wave pattern.

The standing wave pattern continues for frequencies up to 700 MHZ, which is a "turnover point". At frequencies near turnover, the standing wave pattern becomes distorted.

Therefore, the maxima and minima of the standing wave are no longer uniformly distributed. Between 700 and 720 MHZ, a distinct value of the phase constant cannot be found from either the amplitude distribution plot or the relative phase curve. In that frequency band, the behavior of the phase curves are hard to predict. At 720 MHZ, the amplitude distribution shows attenuation and a distinct value of the phase constant can be determined from the relative phase curve. This region goes up to 825 MHZ. Here the structure is an efficient radiator. The phase curve yields a slope from the phase change in degrees per cell. If ϕ is the phase change at the distance d from the first element, then the phase constant β is given by,

$$\beta = \frac{2\pi\phi}{360d}$$

The attenuation per cell in db is also provided from the amplitude plot. However, the data at 875 MHZ shown in Figure III-6 indicates that the structure is approaching a frequency region of standing wave phase and amplitude distribution. Here the attenuation is very low and effective radiation does not occur. This region of low radiation exists up to 1200 MHZ.

Final analysis of the data shown in Figures III-2 through 8 is summarized in the k-β or Brillouin diagram of Figure III-9. It also contains an attenuation curve showing the rate of decay of the wave along the structure as a function of frequency. By inspection of the k-β diagram, an abrupt change is seen in the curve at about

700 MHZ. Here the loops are close to their one-wavelength resonance. At frequencies below this turnover point, the structure acts as a loaded transmission line. The loops are electrically short and the feeder wave propagates along the structure as a slow wave. This section corresponds to the feed excitation region in the log-periodic antenna.

At frequencies above 700 MHZ, the phase velocity of the wave is fast, that is $k>\beta$. The plots of amplitude distribution shows that the rate of attenuation is greatest just above turnover and during this frequency range phase progression is lagging. This corresponds to efficient radiation in the forward direction.

The phase changes from lagging at 825 MHZ to leading at 875 MHZ. This phenomenon is consistent with the transition to backfire directivity. However, in this frequency region the attenuation becomes negligible and as the frequency of excitation is further increased, the wave on the structure is once again of the standing wave type.

To sum up, the propagation region is immediately followed by a strong forward radiation region and then relatively weak backward radiation region. Thus, the tapered version of this array probably will be a poor log-periodic antenna.

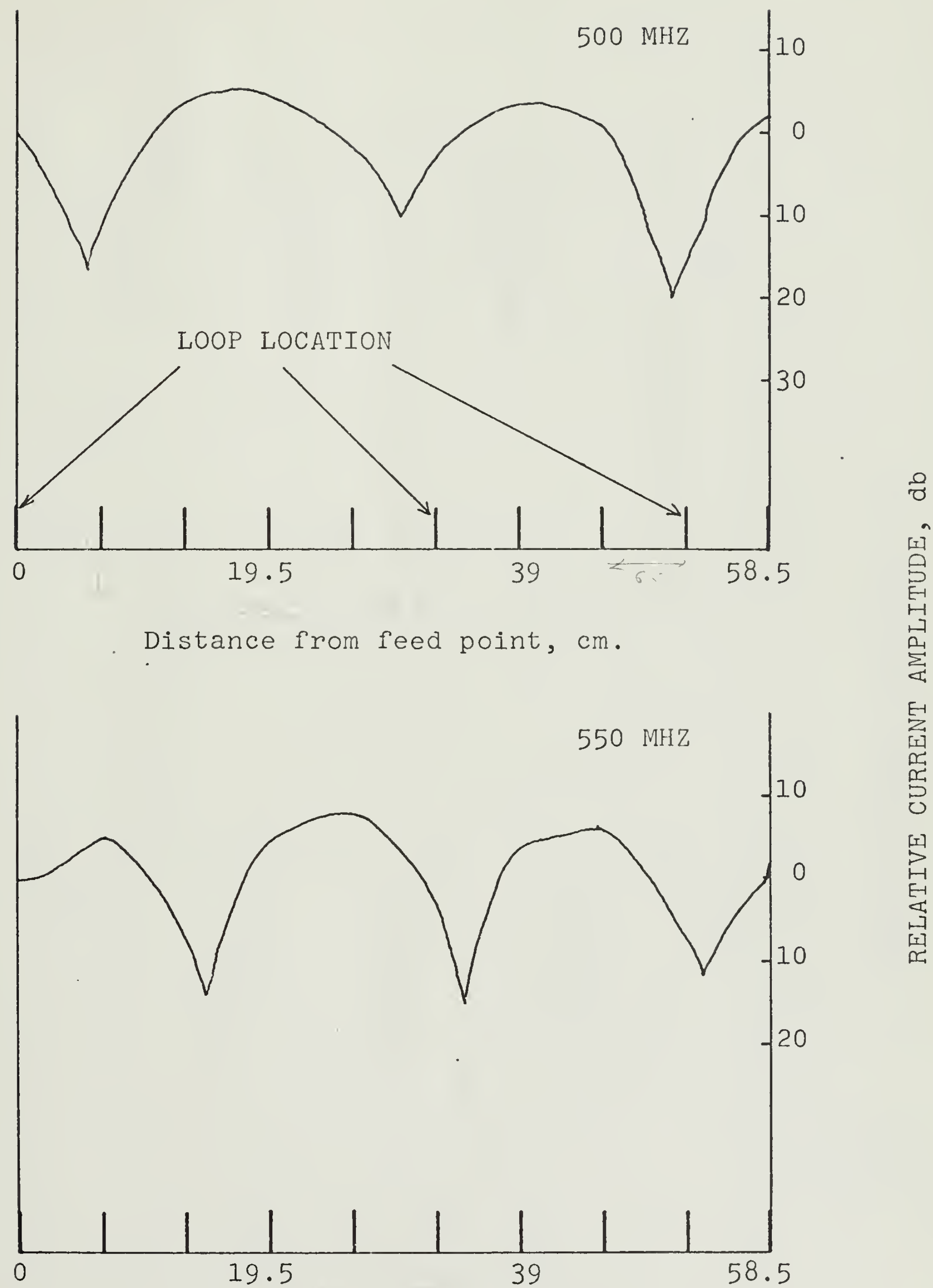

Figure III-2.

Measured amplitude distributions for Type A antenna.

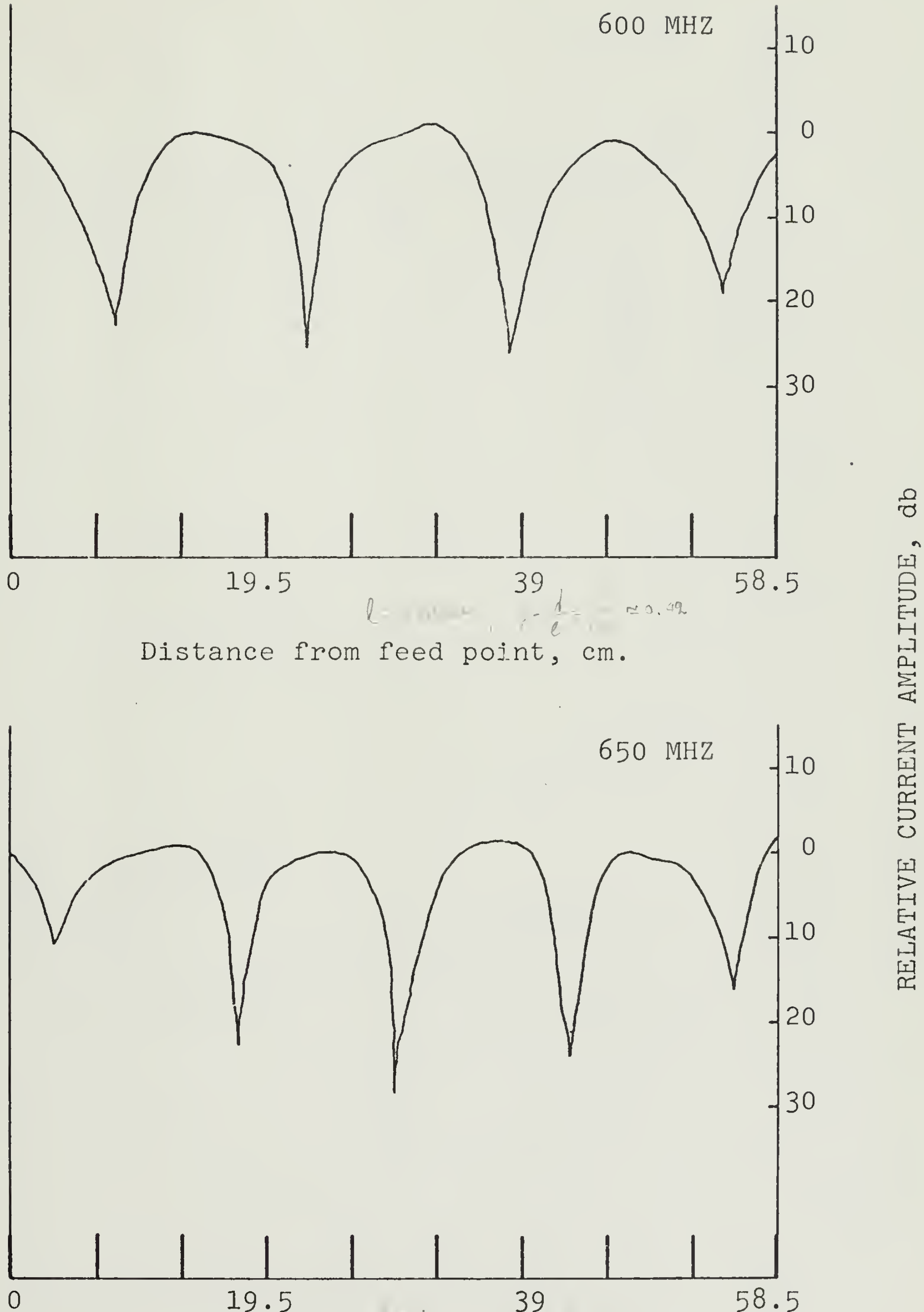

Figure III-3.

Measured amplitude distributions for Type A antenna.

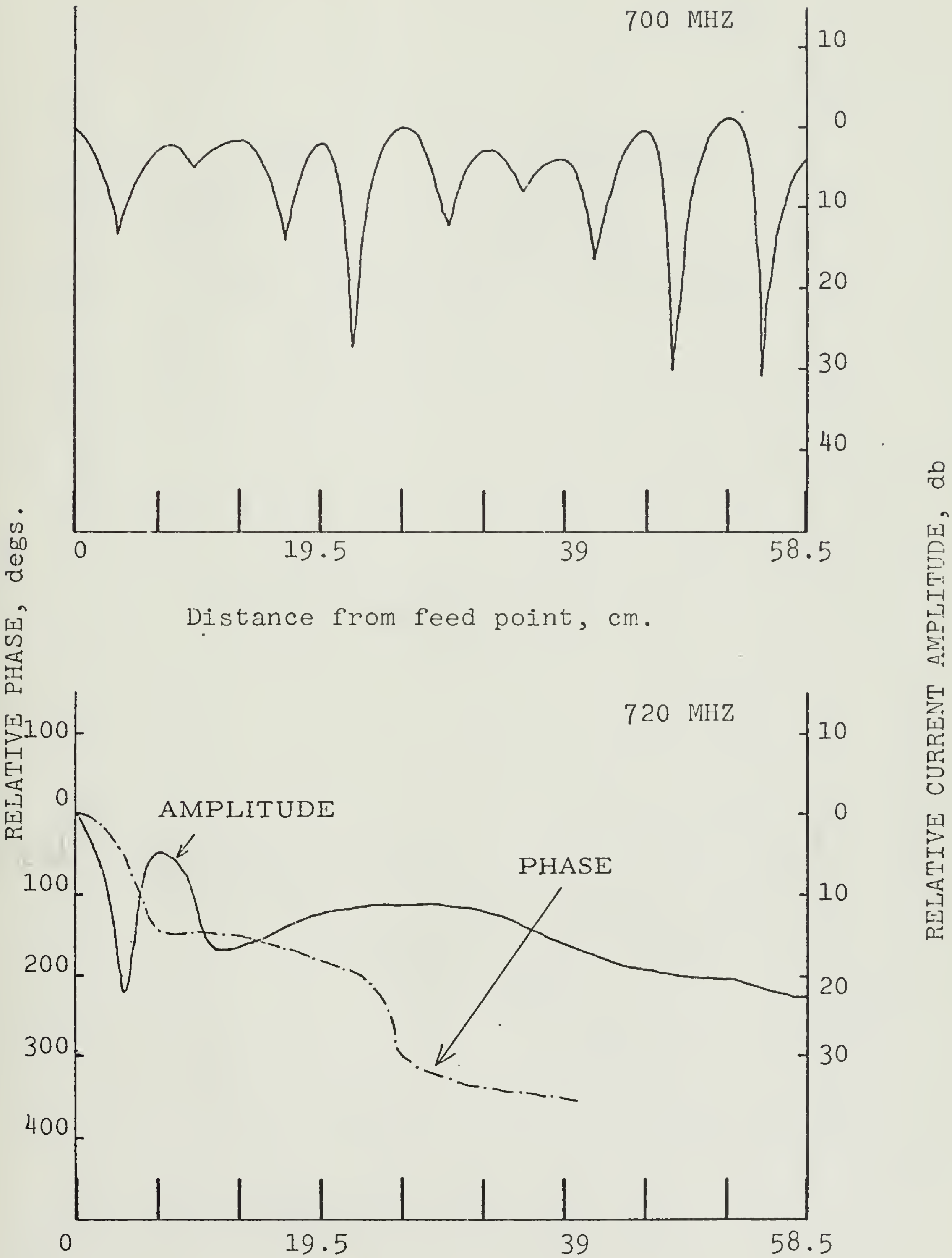

Figure III-4.

Measured amplitude and phase distribution for Type A antenna.

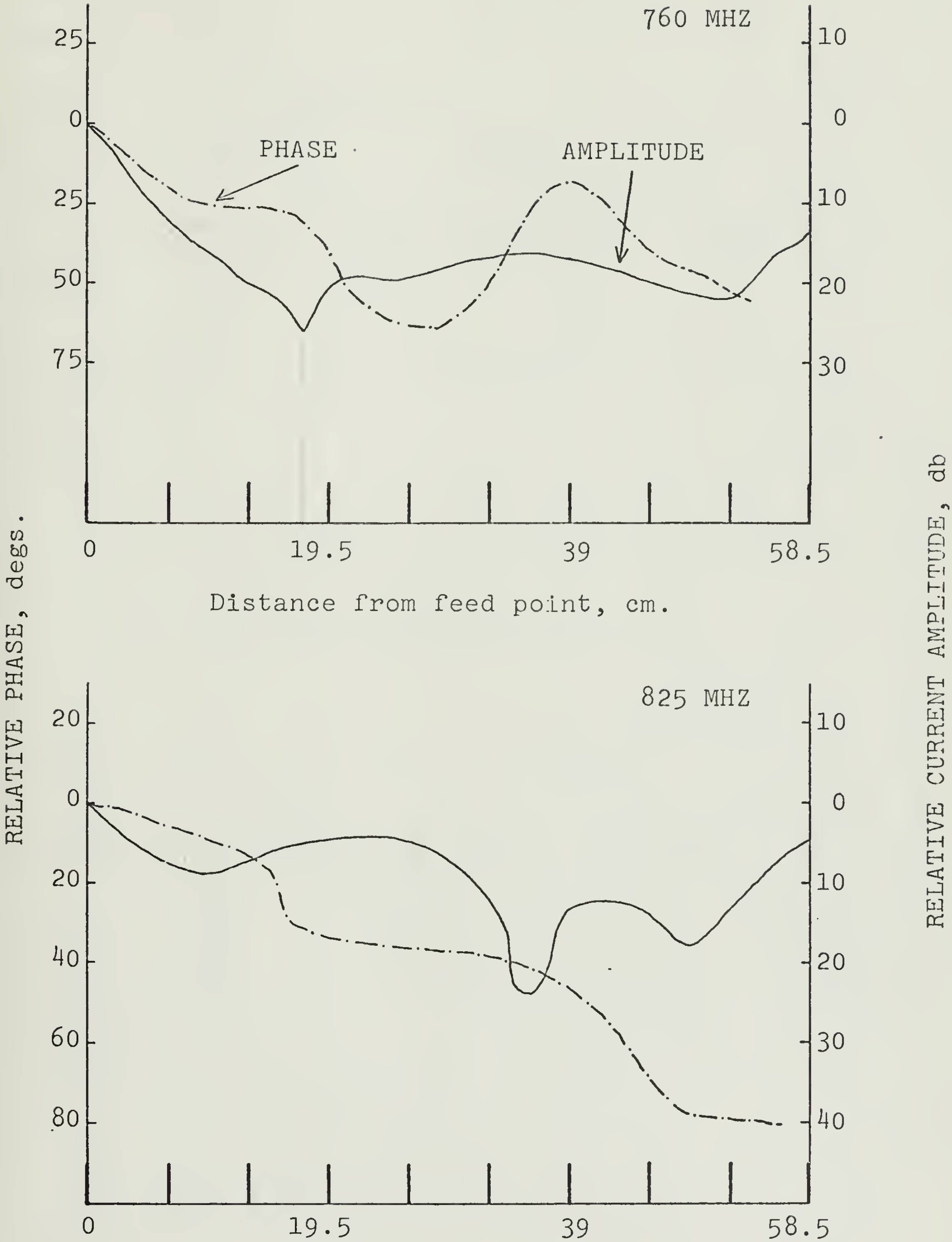

Figure III-5.

Measured amplitude and phase distribution for Type A antenna.

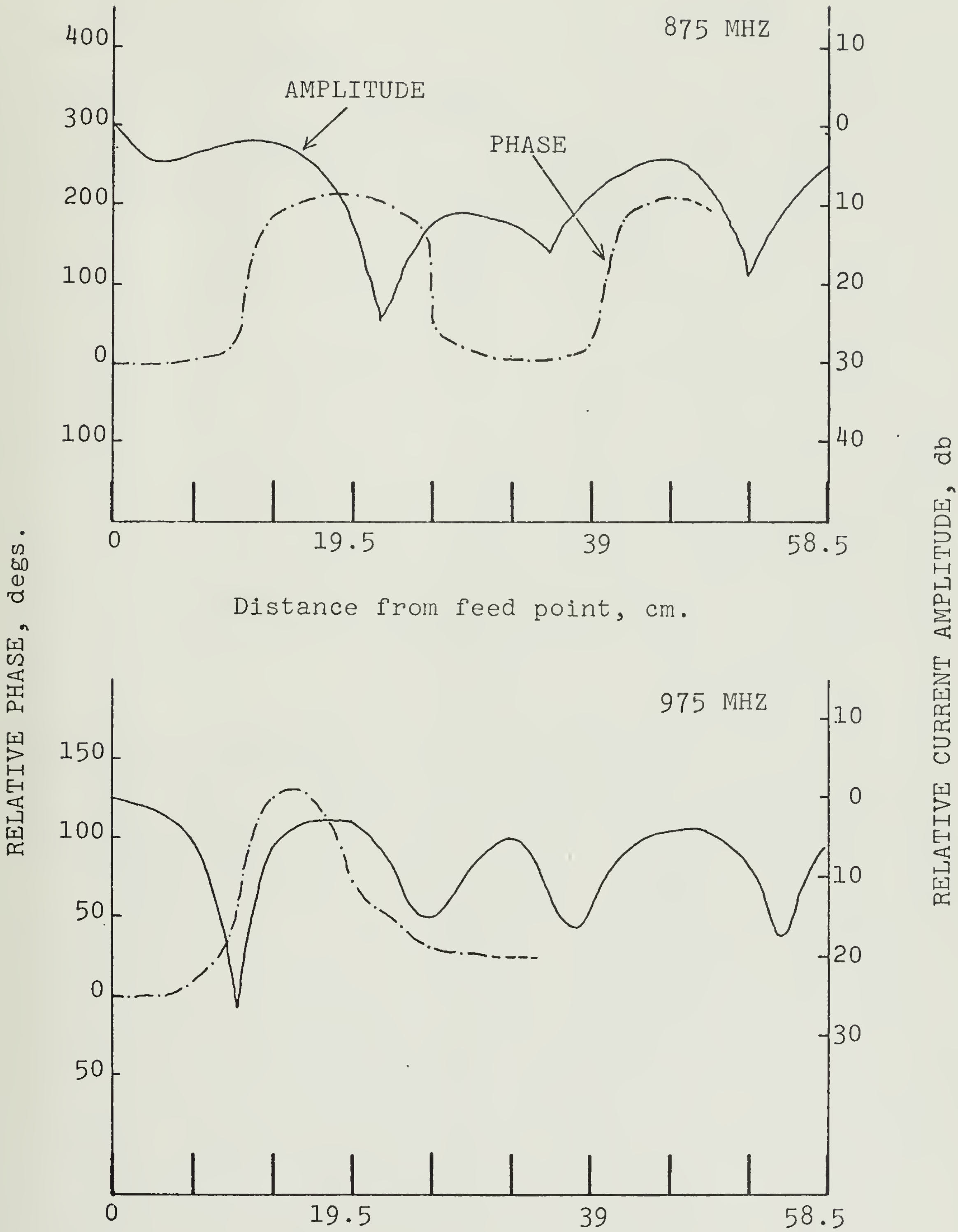

Figure III-6.

Measured amplitude and phase distribution for Type A antenna.

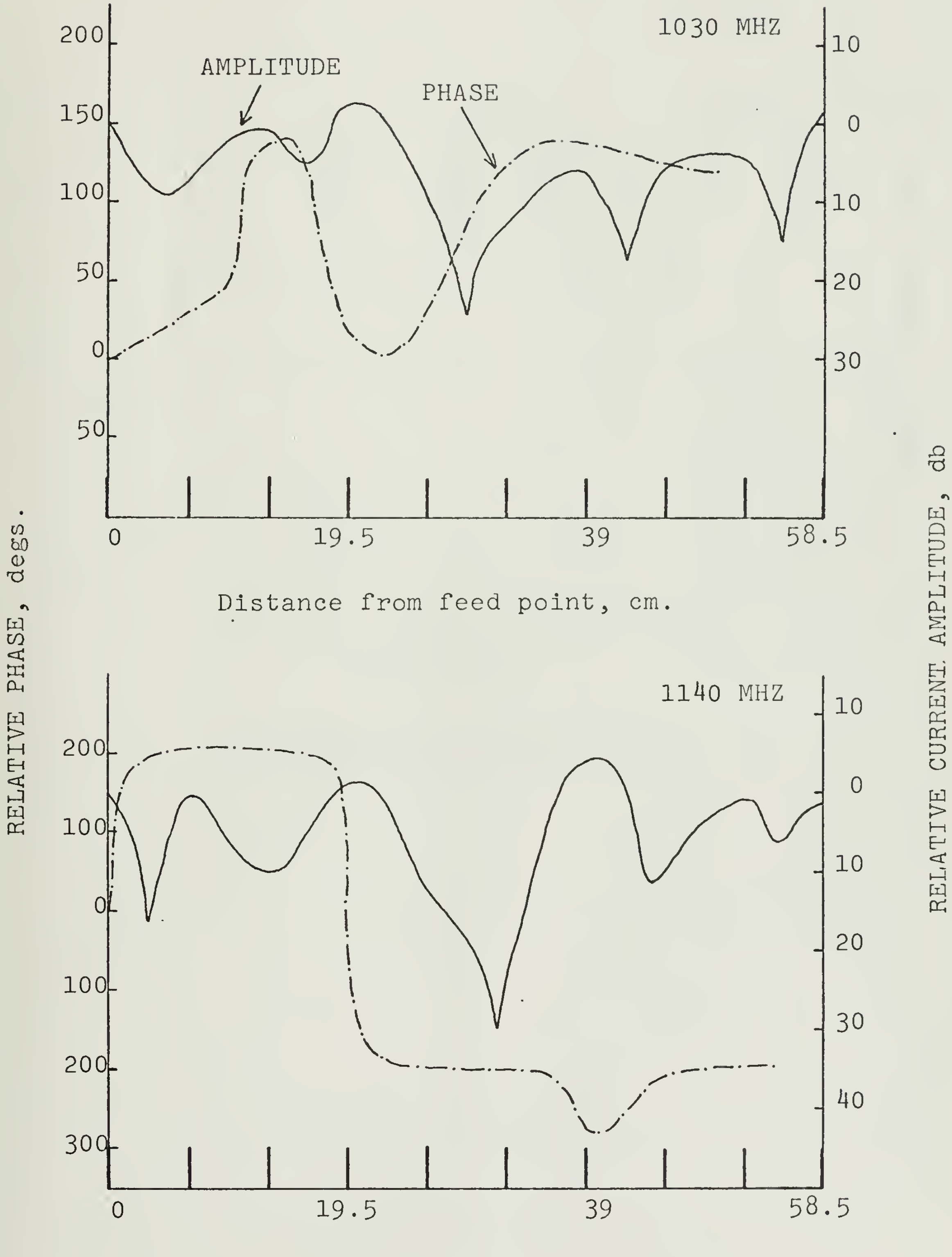

Figure III-7.

Measured amplitude and phase distribution for Type A antenna.

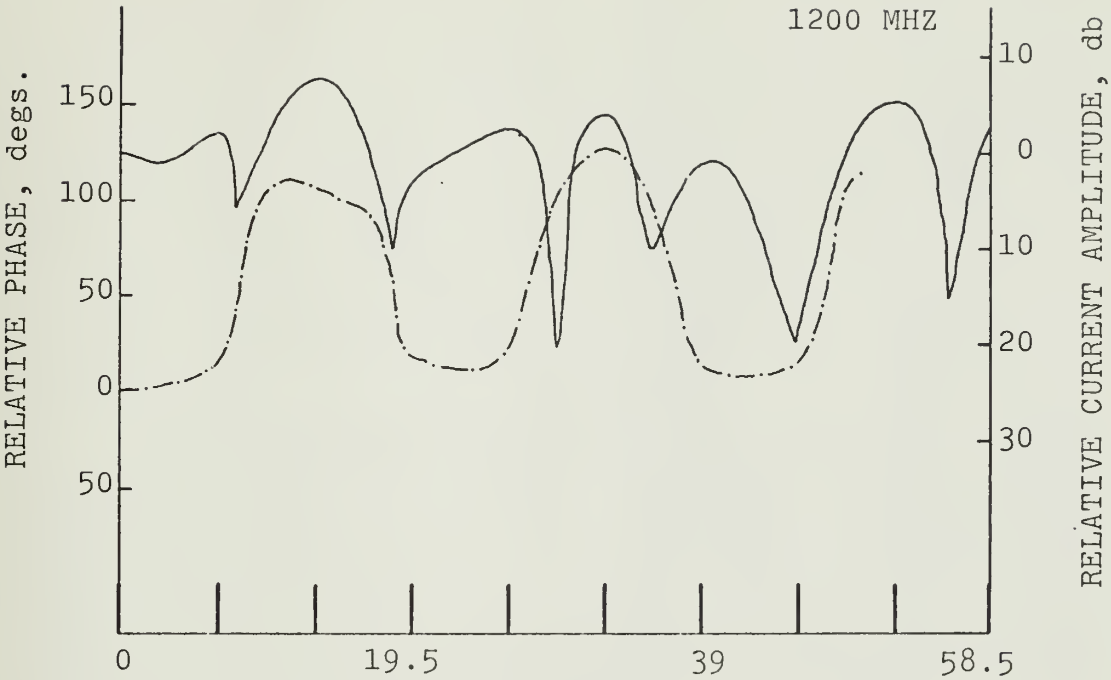

Distance from feed point, cm.

Figure III-8.

Measured amplitude and phase distribution for Type A antenna.

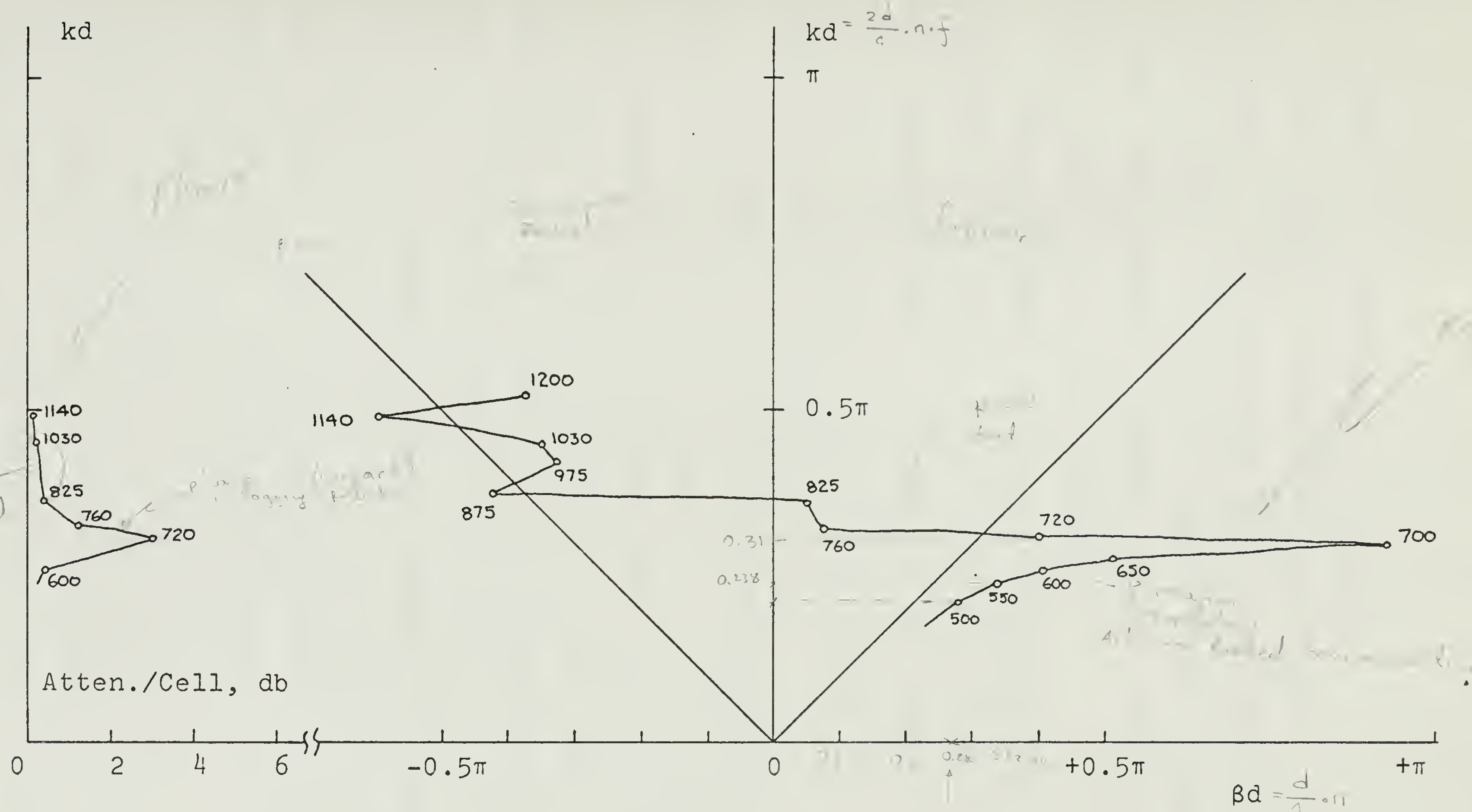

Figure III-9.

The k-β/attenuation diagram for Type A antenna.

B. TYPE B - UNIFORM ARRAY (REVERSED)

This antenna is shown in Figure III-10. It differs from Type A, just discussed, only by the feed mechanism. In this array, the loops are placed along a transposed feeder. This method of feeding clearly introduces a 180 degree phase shift between elements.

The experimental data and corresponding k-β and attenuation diagrams are shown in Figures III-11 through 17. The frequency range is the same for both types. The technique for obtaining all data and the manner of the presentation of results are identical.

By inspection of the current amplitude/phase distribution curves and the corresponding k-β/attenuation diagrams, it is immediately seen that the wave supported on the structure is of the form of a standing wave and experiences no attenuation up to 550 MHZ. Here propagation constant is determined from the standing wave pattern. In fact, 550 MHZ is the propagation constant turnover frequency. At frequencies above turnover, up to 620 MHZ, the standing wave pattern becomes distorted and the progression of phase is lagging. This would correspond to radiation in the forward direction, but on the other hand, an inspection of the attenuation curve shows negligible attenuation in this frequency region. In this frequency band, the propagation constants are determined from corresponding phase curves.

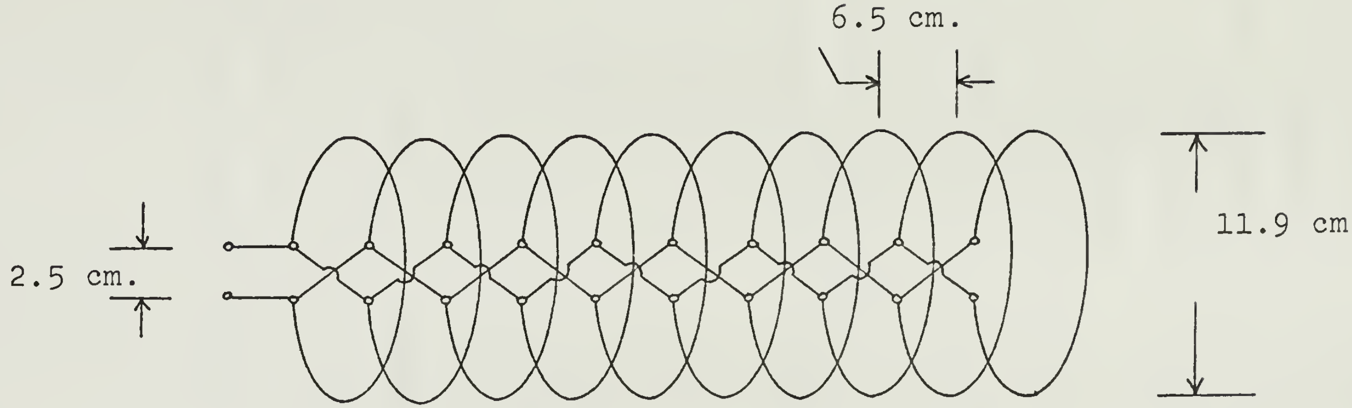

Figure III-10.

TYPE B - Uniformly periodic loop antenna (reversed).

At 620 MHZ, the phase changes from lagging to leading and the attenuation becomes significant. The plots of amplitude distribution shows that the rate of attenuation is greatest between 675 and 800 MHZ which corresponds to an efficient radiation in the backward direction. As the frequency of excitation is increased up to 1000 MHZ, the wave on the structure becomes a standing wave and attenuation is negligible.

Further increase in frequency results in amplitude distributions being fairly smooth. The phase still leads on the structure. However, at 1070 MHZ, the attenuation becomes very high again. It is expected therefore that the structure should be radiating and predominately in the backfire direction.

In summary, the uniform array has a continuous slow-wave propagation region, immediately beyond which it moves into a very efficient backward radiation range. Therefore, the log-periodic counterpart of this structure probably will be a successful frequency independent antenna.

Since the backward radiation is quite efficient it is not important what the k-β properties of the structure are beyond the radiation region.

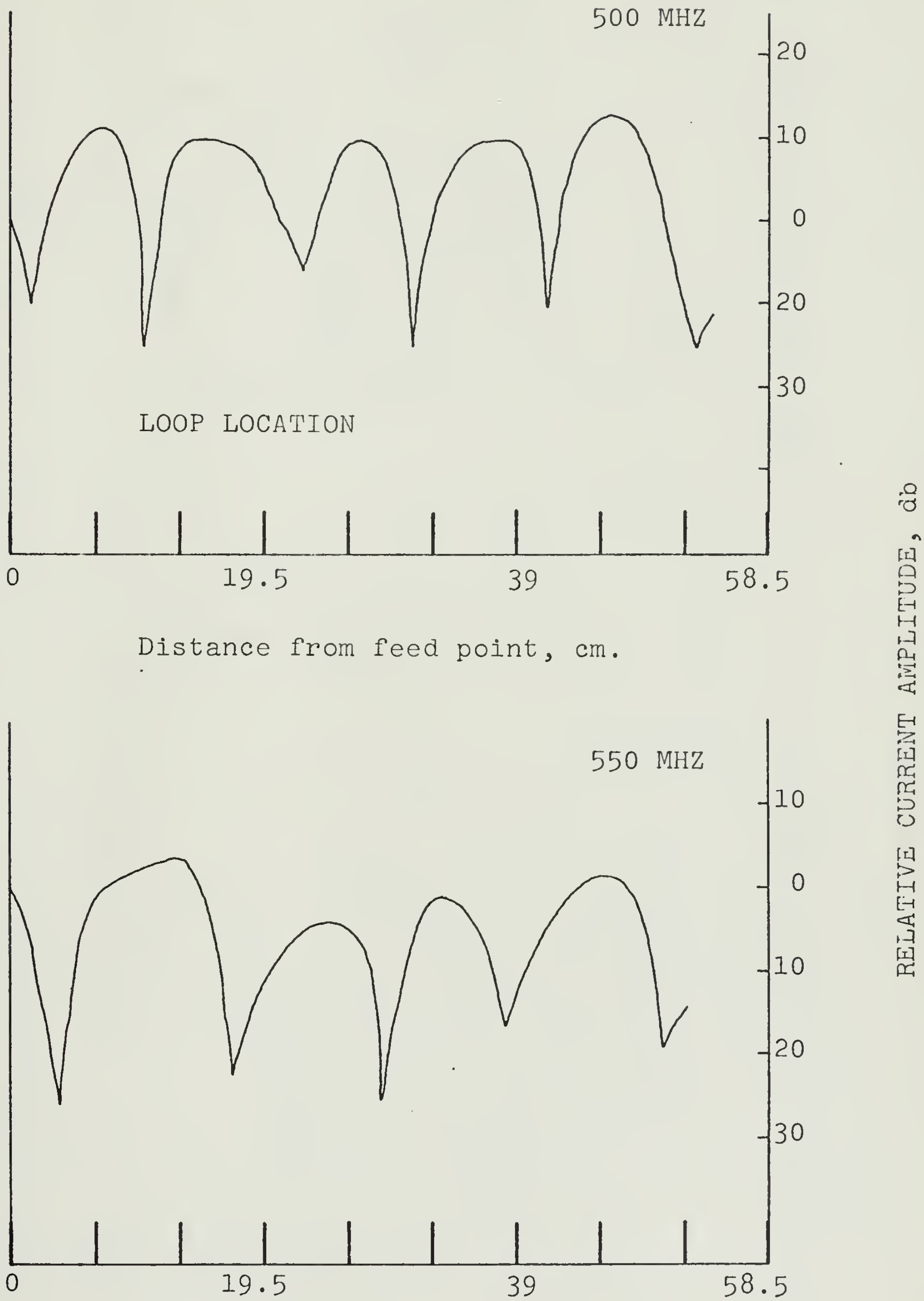

Figure III-11.

Measured amplitude distribution
for Type B antenna.

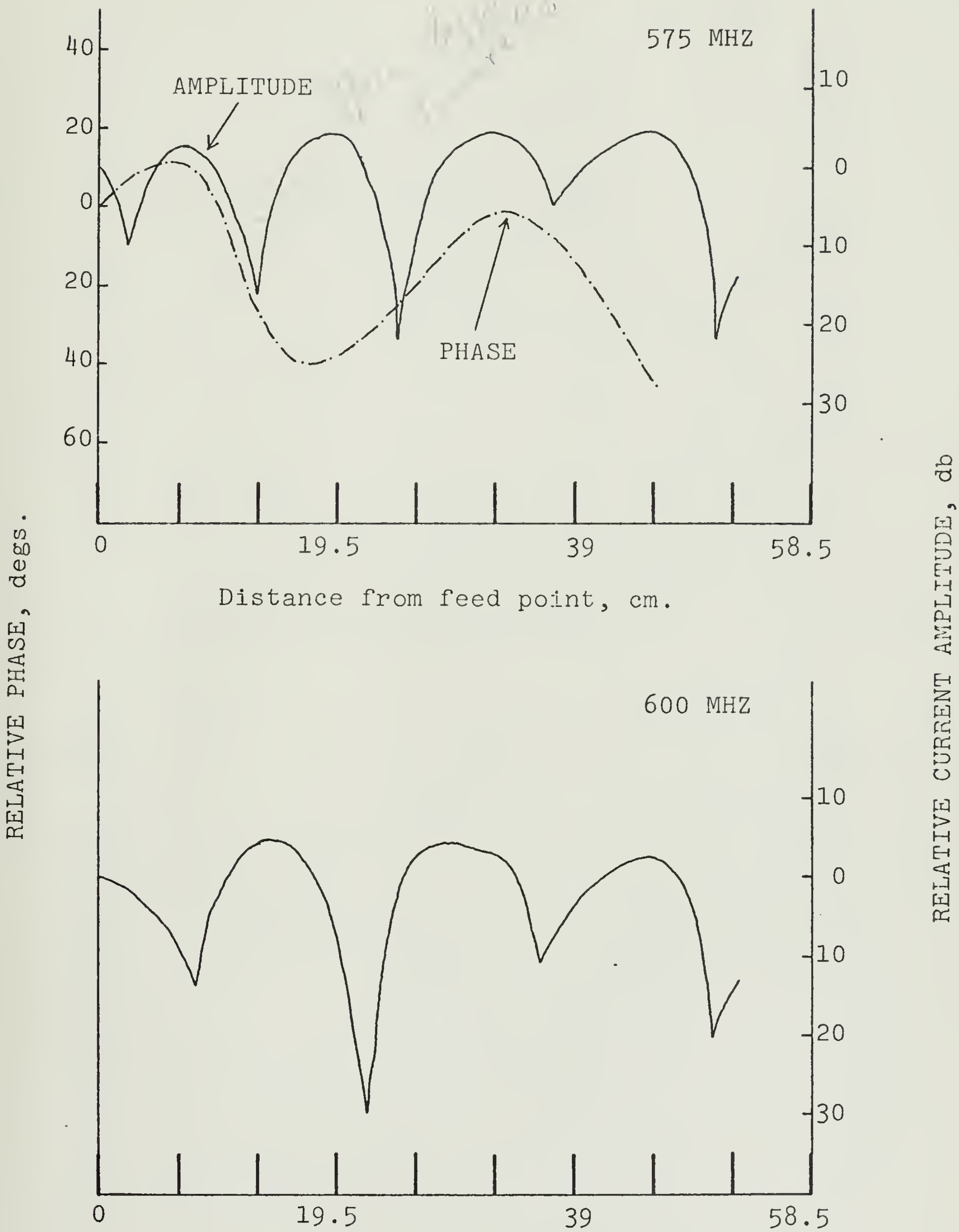

Figure III-12.

Measured amplitude and phase
distribution for Type B antenna.

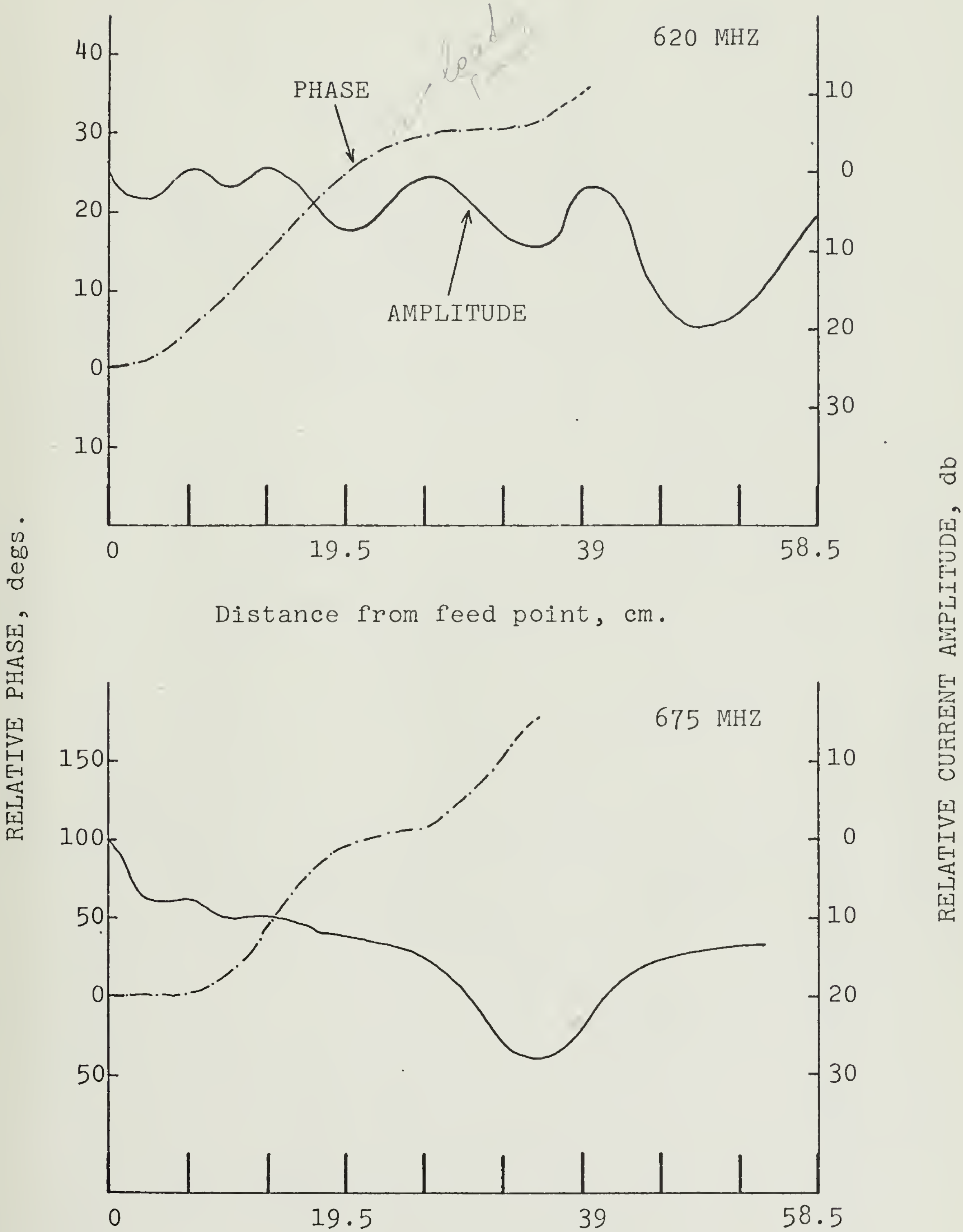

Figure III-13.

Measured amplitude and phase distribution for Type B antenna.

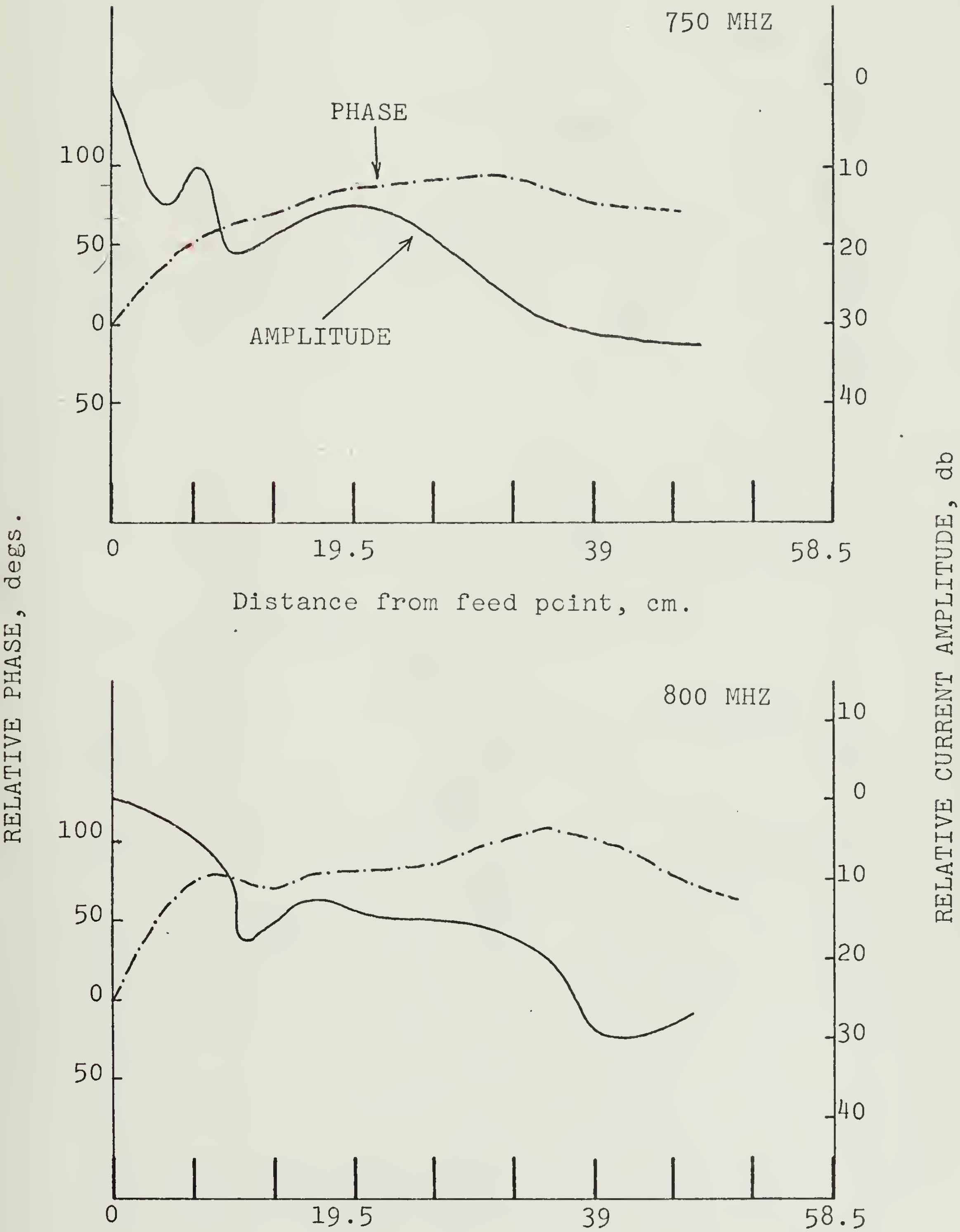

Figure III-14.

Measured amplitude and phase distribution for Type B antenna.

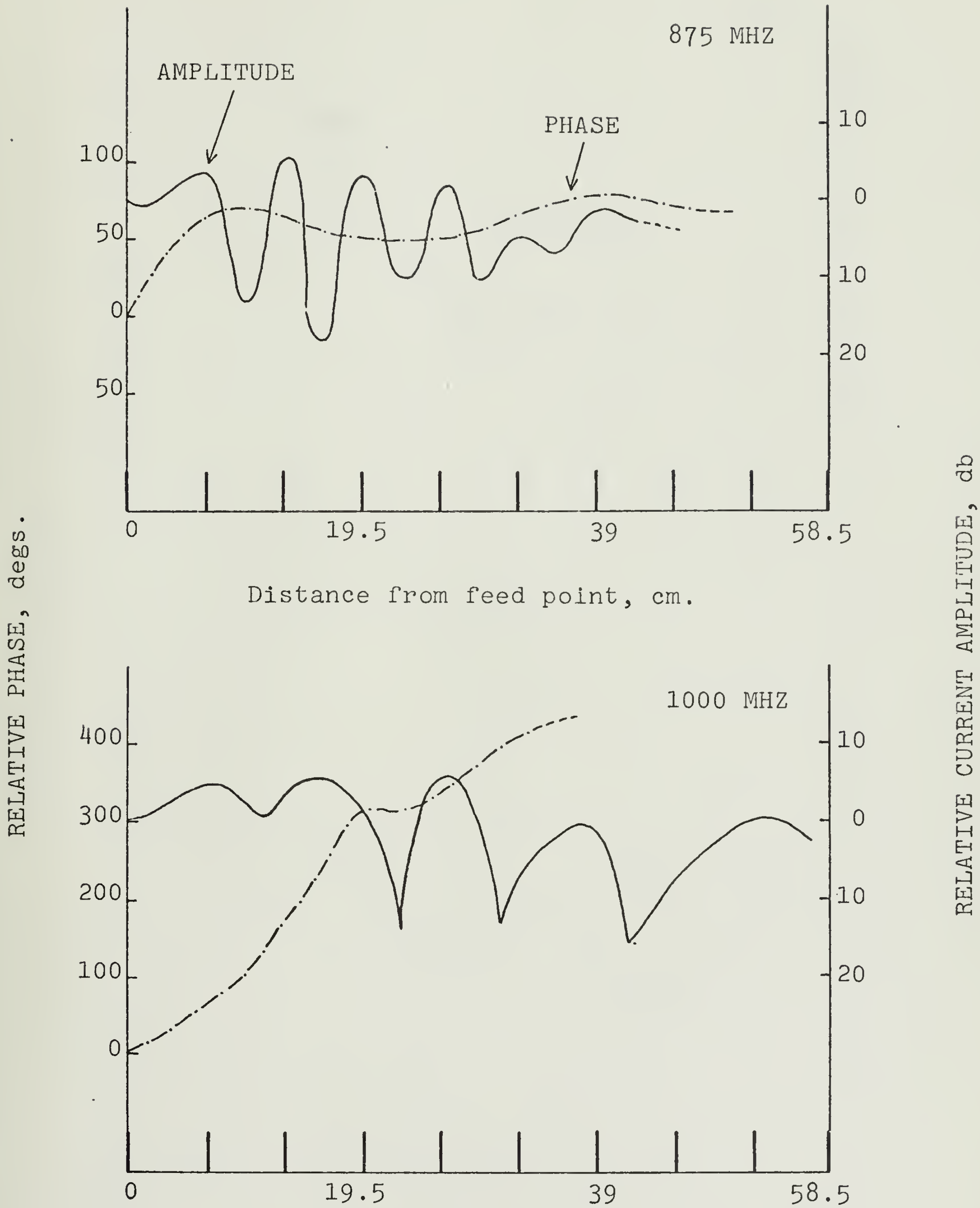

Figure III-15.

Measured amplitude and phase distribution for Type B antenna.

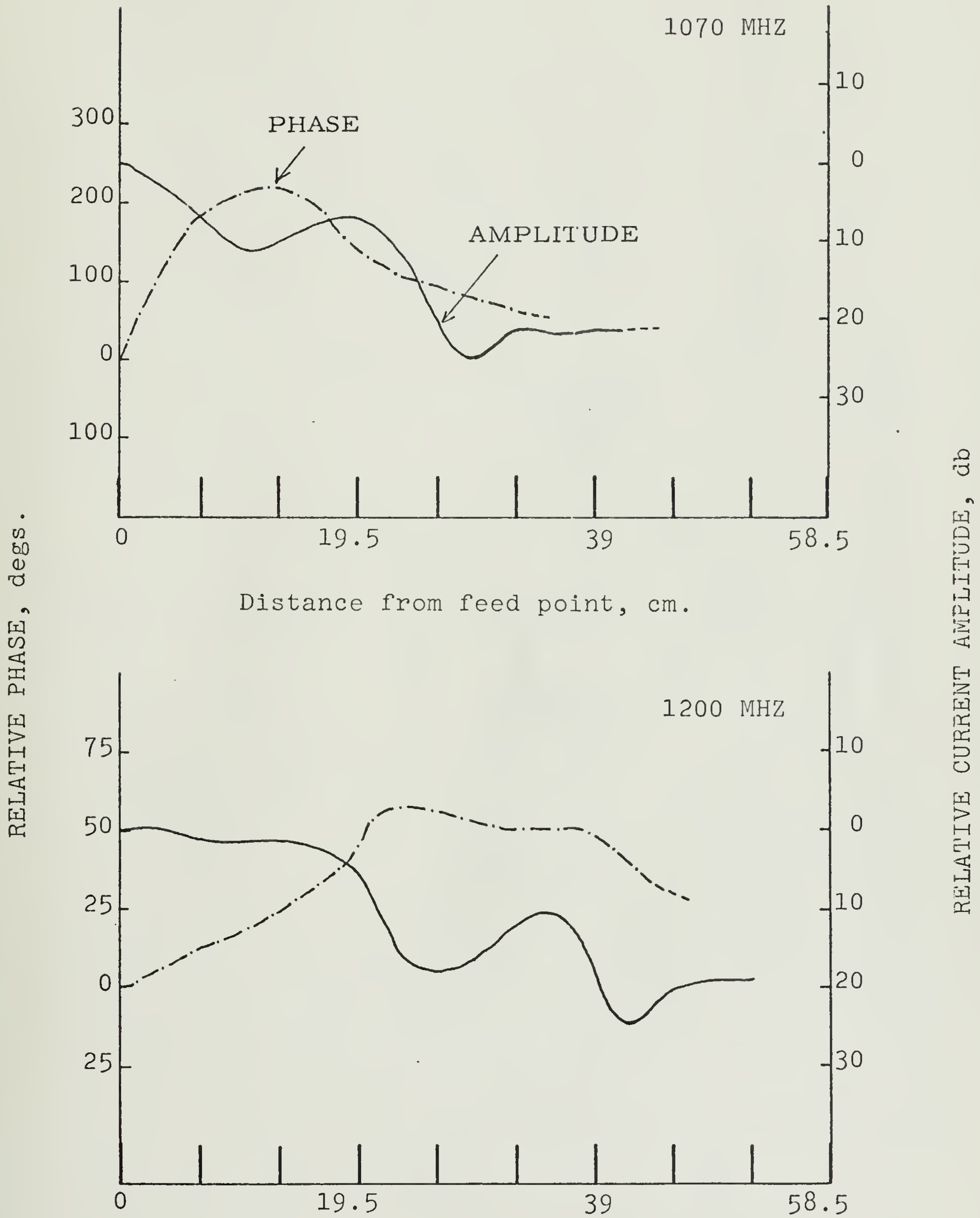

Figure III-16.

Measured amplitude and phase distribution for Type B antenna.

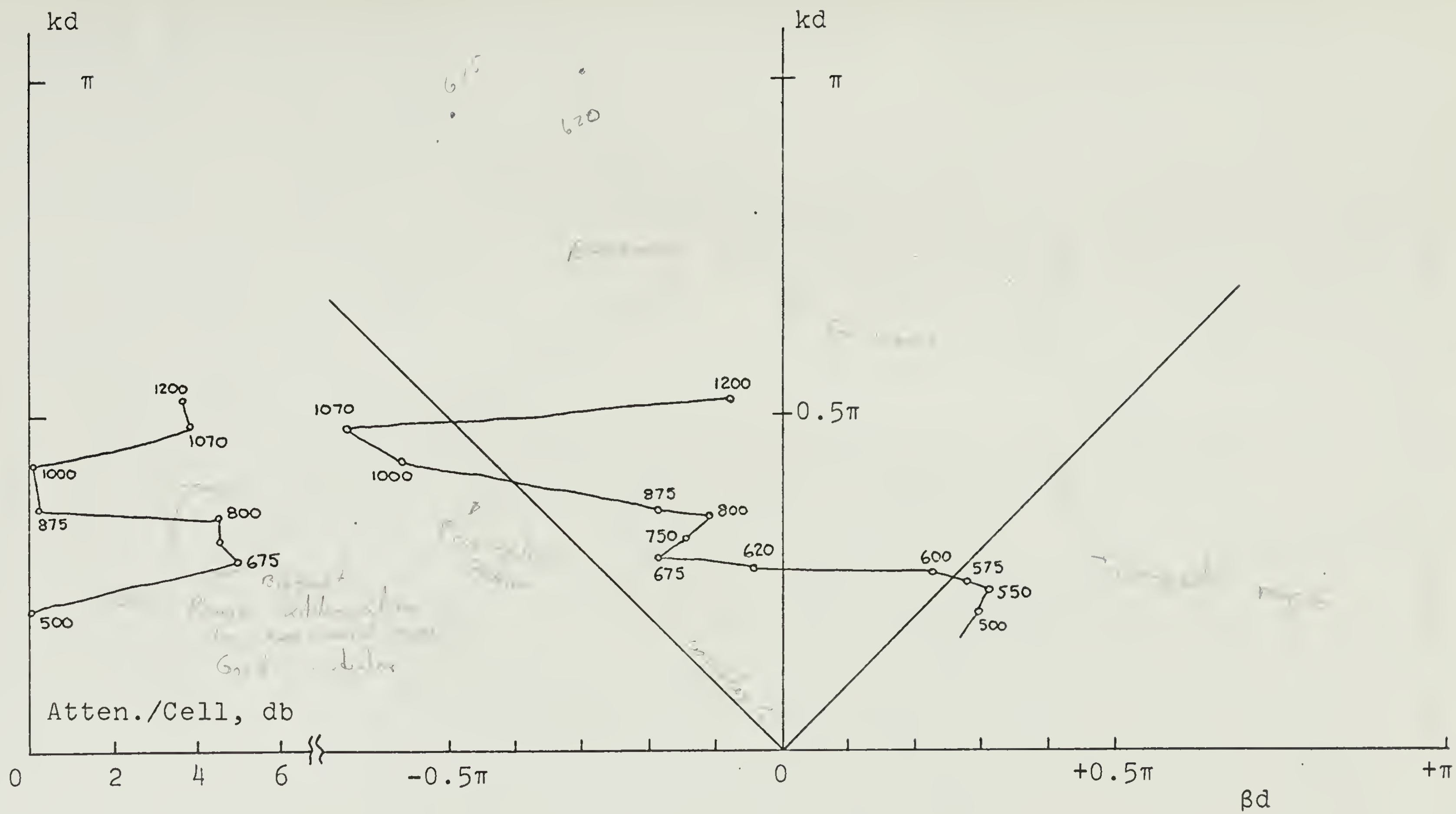

Figure III-17.

The k-β/attenuation diagram for Type B antenna.

IV. CONCLUSIONS AND RECOMMENDATIONS

The purpose of this thesis was to investigate the near field characteristics of uniformly periodic loop arrays to obtain insight into the possibility of a successful log-periodic loop array. This objective was accomplished by use of Brillouin diagram analysis for open structures. The Brillouin (k-β) diagrams for the uniformly periodic loop array have been determined experimentally for the unreversed and alternately reversed cases.

It was seen from the data that the character of the phase distribution along the structure, particularly over the first cell or two, indicated the directional properties of the structure. That is, if the phase of the wave on the structure was leading over the first cell or two, even if the amplitude distribution corresponds to a standing wave, distinct backward directivity was established. For the 875 to 1200 MHZ band, this phenomenon can be seen from the curves of the Type A antenna (see Figures III-6 through 8). An arbitrary reference point, on the standing wave pattern of the amplitude distribution, moves toward the feed point of the structure with increasing frequency. This corresponds to a leading phase distribution along the structure. However, effective radiation does not take place unless the excitation wave undergoes substantial decay with distance along the array.

An effective backward radiation region, preceded by a continuous propagation region, was the distinguishing

property of the alternately transposed loop-loaded structure. The establishment of this condition is imperative for achieving successful frequency independent antenna design.

The d-β diagram of the unreversed loop-loaded structure begins with a propagation region and immediately shifts into an effective forward radiation region. Since forward-directed radiation is an inherent trait in many known unsuccessful log-periodic antennas, this structure is not expected to be a successful broadband antenna.

Inspection of the k-β diagram of the reversed loop-loaded structure shows that the most effective backward radiation takes place in the 620 to 800 MHZ region. Therefore, with this type of feed, a log-periodic loop antenna can be constructed about a center frequency of 710 MHZ, by using the original element of the uniformly periodic array as the center element of the log-periodic form, and by setting the axial spacing between the fifth and sixth elements in the log-periodic structure approximately equal to the spacing of the uniformly periodic array. The choice of appropriate τ and α determines the upper and lower band limits.

In this investigation, the reversed loop-loaded type structure geometry was chosen without performing any calculations. The dimensions of well-known conventional type log-periodic antennas, monopole or dipole arrays, were the starting point of the dimensions of the uniformly periodic loop array. Therefore, it cannot be claimed that this

particular antenna has been optimized. Different spacings or loop sizes may yield more desirable results. A theoretical analysis and then experimental demonstration of the uniformly periodic counterpart of the proposed log-periodic tapered antenna are suggested as initial steps in the development of the broadband structure. The next step is a theoretical analysis of the log-periodic antenna which will decrease the effort and time required to achieve a successful antenna design.

The last step is to construct the log-periodic antenna and to test its performance.

APPENDIX A: A BROADBAND PRINTED CIRCUIT BALUN

Many antennas that are used in practice are "balanced" with respect to ground. However, usually one uses coaxial lines to feed these structures. The conductors in coaxial lines are "unbalanced" with respect to ground.

A balun is a device that transforms the field structure of an unbalanced transmission line to that of a balanced transmission line. There are numerous baluns [13, 14] which can be used over a wide frequency range. A new type of printed circuit balun which is particularly well suited to wideband applications was used in this investigation. This balun is easy to construct and is compact.

It is similar to the one designed by Bawer and Wolfe and it is illustrated in Figure A-1. The top and bottom views indicate the simplicity of the balun's construction.

Here, the unbalanced input consists of a thin conductor etched on the bottom side of the dielectric sheet. The copper on top of the dielectric serves as a ground plane for the unbalanced input conductor. A balanced output for the antenna appears at the terminals X and X' as shown in the top view.

Length, θ_b, in the balun is about a quarter wavelength at the midband frequency. For proper transformation it is required that $Z_b = R^2/Z_{ab}$, where Z_{ab} is the impedance of

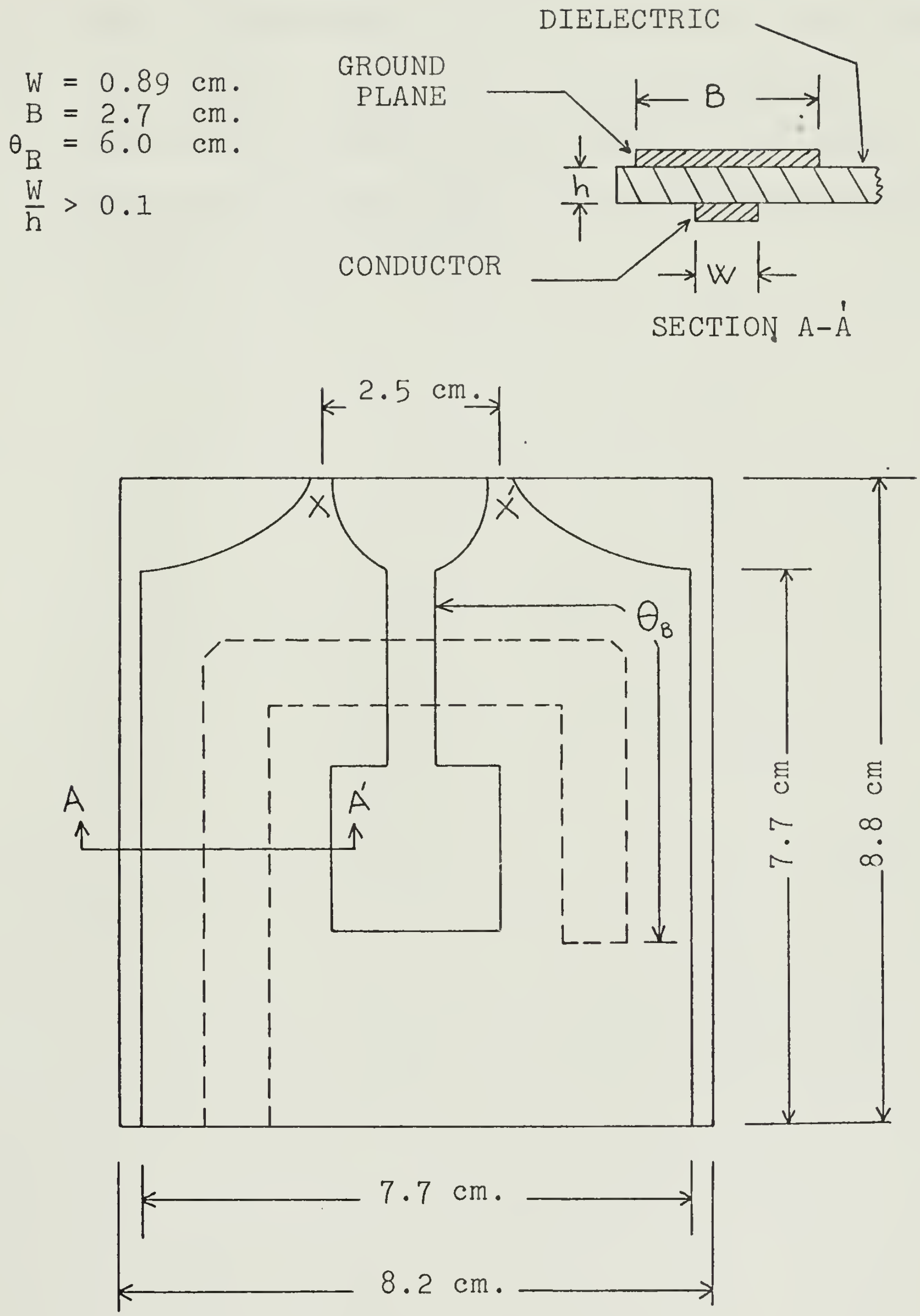

Figure A-1.

Illustration of the construction of a printed circuit balun.

the wide parallel line, R is the load resistance and Z_b is the characteristic impedance of the unbalanced input line.

A printed circuit board with dielectric constant $\varepsilon_R = 2.53$ was used to construct the device. For dimensional calculations of the balun, the wide strip approximation [16] ($W/h > .1$) was sufficient.

BIBLIOGRAPHY

1. Dyson, J. D., "Frequency-Independent Antennas", Electronics, pp. 39-44, April 20, 1962.

2. Weeks, W. L., Antenna Engineering, McGraw-Hill Book Co., Inc., New York, 1968.

3. Isbell, D. E., "Log-Periodic Dipole Arrays", IRE Trans. on Antennas and Propagation, Vol. AP-8, pp. 260-267, May 1960.

4. Carrel, R. L., Analysis and Design of the Log-Periodic Dipole Antenna, Tech. Rp. No. 52, Contract AF 33(616)-6079, Antenna Lab., University of Illinois, October 1961.

5. Carrel, R. L., "The Design of Log-Periodic Dipole Antennas", IRE National Conv. Record, Part I, pp. 61-75, 1961.

6. Jones, K. E., and Mittra, R., A Study of Continuously Scaled and Log-Periodically Loaded Transmission Lines, presented in URSI Meeting in Ottawa, Fall, 1962.

7. Mayes, P. E., Deschamps, G. A., and Patton, W. T., "Backward Wave Radiation from Periodic Structures", Proc. IRE, Vol. 49, No. 5, May 1961.

8. Mittra, R., and Jones, K. E., "Theoretical Brillouin (k-β) Diagrams for Monopole and Dipole Arrays and Their Application to Log-Periodic Antennas", IEEE Trans. on Antennas and Propagation, Vol. AP-12, pp. 533-540, September 1964.

9. Lindsay, J. E., Jr., "A Parasitic End-Fire Array of Circular Loop Elements", P.G.A.P., pp. 697, September 1967.

10. Laxpati, Unpublished work.

11. Mayes, P. E., and Ingerson, P. G., "Near-Field Measurements on Backfire Periodic Dipole Arrays", Proceedings of 12th Annual Symposium, USAF Antenna Research, Allerton Park, Illinois, 1962.

12. Hudock, E., Near-Field Investigation of Uniformly Periodic Monopole Arrays, Tech. Rp. No. 1, Antenna Lab., University of Illinois, May 30, 1963.

13. Roberts, W. K., "A New Wide-Band Balun", Proc. IRE, Vol. 45, pp. 1628-1631, December 1957.

14. McLaughlin, J. W., Dunn, D. A., and Grow, R. W., "A Wide-Band Balun", IRE Trans. on Microwave Theory and Techniques, Vol. MTT-6, pp. 314-316, July 1958.

15. Bawer, R., and Wolfe, J. J., "A Printed Circuit Balun for Use With Spiral Antennas", IRE Trans. on Microwave Theory and Techniques, Vol. MTT-8, pp. 319-324, May 1960.

16. The Microwave Engineers' Handbook and Buyers' Guide, Horizon House, Dedham, MA., pp. 94-95, 1968.

INITIAL DISTRIBUTION LIST

		No. Copies
1.	Defense Documentation Center Cameron Station Alexandria, Virginia 22314	2
2.	Library Code 0212 Naval Postgraduate School Monterey, Califronia 93940	2
3.	Professor R. W. Adler Department of Electrical Engineering Naval Postgraduate School Monterey, California 93940	3
4.	Lt. Ersan Tezmen, TURKISH NAVY Hunkarimami Hasimbey Sok. 31/7 Kadikoy, Istanbul Turkey	2
5.	Istanbul Teknik Üniversitesi Elektrik Fakültesi Taskisla, Istanbul Turkey	1
6.	Orta-Dogu Teknik Üniversitesi Elektrik Fakültesi Ankara, Turkey	1
7.	Karadeniz Teknik Üniversitesi Elektrik Fakültesi Trabzon, Turkey	1
8.	Deniz Kuvvetleri Komutanligi Personel Egitim Sb. Müdürlügü Ankara, Turkey	1
9.	Deniz Harb Okülü Komutanligi Heybeliada, Istanbul Turkey	1
10.	Deniz Makine Sinif Okullari Komutanligi Derince, Kocaeli Turkey	1
11.	R. T. Leitner, Director of Engineering Technical Appliance Corp. Sherburne, New York 13460	1

12. Professor S. R. Laxpati 1
Department of Information Engineering
University of Illinois at Chicago Circle
P. O. Box 4343
Chicago, Illinois 60680

UNCLASSIFIED
Security Classification

DOCUMENT CONTROL DATA - R & D

(Security classification of title, body of abstract and indexing annotation must be entered when the overall report is classified)

1. ORIGINATING ACTIVITY (Corporate author) Naval Postgraduate School Monterey, California 93940	2a. REPORT SECURITY CLASSIFICATION Unclassified 2b. GROUP
3. REPORT TITLE A Near-Field Investigation of Two Uniformly Periodic Loop Arrays	
4. DESCRIPTIVE NOTES (Type of report and inclusive dates) Master's Thesis, December 1970	
5. AUTHOR(S) (First name, middle initial, last name) Ersan Tezmen	

6. REPORT DATE	7a. TOTAL NO. OF PAGES	7b. NO. OF REFS
December 1970	67	16

8a. CONTRACT OR GRANT NO.	9a. ORIGINATOR'S REPORT NUMBER(S)
b. PROJECT NO.	
c.	9b. OTHER REPORT NO(S) (Any other numbers that may be assigned this report)
d.	

10. DISTRIBUTION STATEMENT

This document has been approved for public release and sale; its distribution is unlimited.

11. SUPPLEMENTARY NOTES	12. SPONSORING MILITARY ACTIVITY
	Naval Postgraduate School Monterey, California 93940

13. ABSTRACT

The k-β diagrams for two different uniformly periodic loop antenna arrays are determined from measured near field amplitude and phase distributions of waves traveling on the structures.

It is found that there are frequency regions where these structures function as effective radiators. The directional characteristics of the radiated fields depend upon the relative phase and amplitude distributions of the near fields.

The k-β diagrams of these periodic antennas are used to predict the behavior of their tapered broadband versions.

The results of this study demonstrate that providing appropriate conditions of phasing are met, backfire radiation can be established and, in turn, a successful broadband antenna can be designed.

DD FORM 1 NOV 65 1473 (PAGE 1)

S/N 0101-807-6811

UNCLASSIFIED
Security Classification

A-31408

14. KEY WORDS	LINK A		LINK B		LINK C	
	ROLE	WT	ROLE	WT	ROLE	WT
Arrays						
Antenna Arrays						
Antennas						
Electromagnetic fields						
Loop Antennas						

Thesis
T35 Tezmen 126115
c.1
A near-field investigation of two uniformly periodic loop arrays.